R. & M. No. 3144

R. & M. No. 3144
(19,902, 20,016)
A.R.C. Technical Report

MINISTRY OF AVIATION

AERONAUTICAL RESEARCH COUNCIL
REPORTS AND MEMORANDA

Investigations on an Experimental Air-Cooled Turbine

Part III.—The Effects of Cooling on the Overall Turbine Aerodynamic Performance and Initial Operation at an Inlet Gas Temperature of 1400 deg K

By D. E. FRAY and N. E. WALDREN

Part IV.—Examination of Sintered Vitallium Air-Cooled Turbine Blades Following 100 Hours' Operation at a Turbine Inlet Mean Gas Temperature of 1400 deg K

By N. E. WALDREN and C. J. HART

LONDON: HER MAJESTY'S STATIONERY OFFICE
1960
PRICE 18s. 0d. NET

Investigations on an Experimental Air-Cooled Turbine

COMMUNICATED BY THE DIRECTOR-GENERAL OF SCIENTIFIC RESEARCH (AIR), MINISTRY OF SUPPLY

---

*Reports and Memoranda No. 3144**
January, 1958

Part III.—The Effects of Cooling on the Overall Turbine Aerodynamic Performance and Initial Operation at an Inlet Gas Temperature of 1400 deg K

By D. E. FRAY and N. E. WALDREN

Summary. Further tests on an experimental air-cooled turbine have been carried out to examine the effect on the turbine aerodynamic performance of cooling-air discharge from the blade tips into the main gas stream. With the design quantities of cooling air applied, a measured loss of efficiency of 2 per cent was recorded. The effect of the nozzle-blade tip clearance of 0·052 in. was also examined, and it is demonstrated that a gain in efficiency of 5 per cent can be realised if this clearance is eliminated.

Initial operation of the turbine at an inlet gas temperature of 1400 deg K for 50 hours is also reported and is shown to be satisfactory.

---

1. *Introduction.* Previous reports[1, 2] have given a general description of an experimental single-stage air-cooled turbine and a detailed account of the cooling characteristics of some internally air-cooled nozzle and rotor blades.

This report deals mainly with the turbine aerodynamic performance and gives an account of the changes in efficiency which arise from the discharge of cooling air into the main gas stream from the tips of the nozzle and rotor blades and from the sheet-metal liners in the turbine inlet section. In addition, the effect of eliminating the clearance space at the tips of the nozzle blades was investigated.

Further rotor-blade cooling characteristics were obtained at higher turbine gas inlet temperatures to determine the variation of blade temperature with cooling-air ratio at higher values of gas temperature to cooling air temperature ratio. Since this entailed increasing the turbine inlet gas temperature to 1400 deg K, a 50 hours' endurance test was carried out at a rotational speed of 8000 r.p.m. At the completion of this test, a strip examination of the turbine was made and details of the condition of the various components are given.

---

* Part III. N.G.T.E. Report R.219, received 19th February, 1958.
Part IV. N.G.T.E. Report R.220, received 24th March, 1958.

2. *Description of Tests.* 2.1. *Tests to Determine the Effect of Cooling-Air Discharge into the Main Gas Stream.* Operation of a turbine at a mean inlet gas temperature of up to 1100 deg C or more necessitates provision of a means of cooling a large part of the turbine structure in addition to the blades. The turbine annulus before the nozzle blades is cooled by forming the annulus walls of sheet metal such that cooling air may be passed underneath these liners (Fig. 1). On the outer diameter wall the cooling air (w_1) passes beneath the liner and is discharged into the main gas stream from an annular gap just ahead of the nozzle guide vanes. On the inner diameter a portion of the cooling air (w_2) is discharged into the main gas stream through a row of holes in the liner to provide additional film cooling for the liner. The remainder of the inner-wall cooling air (w_3) passes underneath the nozzle-shroud liner to be discharged finally into the main gas stream through an annular gap downstream of the nozzle blades.

It may therefore be anticipated that this discharge of cooling air upstream of the blade rows may have a detrimental effect on the main-gas-stream boundary-layer flow at the turbine nozzle and rotor blade roots. In a similar fashion, the ejection of cooling-air flows w_N and w_R at the tips of the nozzle and rotor blades respectively may cause greater secondary losses than without this air discharge. Alternatively it is sometimes argued that this ejection of cooling air will cause an effective reduction in tip clearance by partially 'filling' the clearance space and hence causing an increase in turbine efficiency. These effects, however, are not calculable and must be determined experimentally.

Now when the turbine is operated with combustion, alterations in the nozzle and rotor blade tip clearance can be caused by changes in thermal expansion of various parts of the turbine structure. Therefore, if the injection of cooling air to any part of the turbine is varied, these clearances will change. This, in turn, will cause a change in the overall aerodynamic performance of the turbine stage. During preliminary tests with combustion these changes in clearance due to thermal behaviour were found to mask the changes caused by cooling-air discharge into the main gas stream. The tests were therefore carried out without combustion, with the 'cooling air' at the same temperature as the main gas stream such that the turbine blade tip clearances remained substantially constant. The following cooling-air quantities were then applied independently:

(*a*) Inner annulus liner and nozzle-shroud cooling air ($w_2 + w_3$) .. 2·0 per cent
(*b*) Outer annulus liner cooling air (w_1) .. .. 1·5 per cent
(*c*) Nozzle-blade cooling air (w_N) .. .. 2·0 per cent
(*d*) Rotor-blade cooling air (w_R) .. .. 2·0 per cent .

The quantities are expressed as percentages of the main-gas-stream flow at the point of injection. In addition, the effect of combined injection of these flows was determined.

In each test the turbine was operated at a main-gas-stream Reynolds number on to the rotor blades of 2×10^5 and prior to the application of each separate cooling-air flow a 'datum' test was made with no cooling air. Variation of the turbine rotational speed permitted a wide range of operating incidences on to the rotor blades and the turbine adiabatic efficiency was determined at a number of different incidences for each cooling-flow application.

2.2. *Tests on the Effect of Eliminating the Nozzle-Blade Tip Clearance.* The turbine was assembled initially with a nominal clearance between the nozzle-blade tips and the nozzle-blade tip shroud of 0·052 in. at room temperature and calculations according to the method of Ainley and Mathieson[3] indicated that this would cause a reduction in adiabatic efficiency of the turbine stage of approximately 5 per cent. At the conclusion of the endurance run at 1400 deg K, since the turbine was scheduled for a complete strip examination, it was decided to investigate the effect of eliminating this clearance. The clearance spaces between each nozzle blade and the nozzle-shroud ring were then filled with plasticine shaped to the nozzle-blade profiles.

In order to prevent removal of the plasticine during the test, it was necessary to carry out the test at as low a temperature as possible and by cooling the air supply to the turbine to the maximum by means of the plant compressor after-cooler, an inlet temperature of 35 deg C was obtained. Prior to applying the plasticine, a datum test was carried out (without cooling-air injection) at this low inlet temperature and at gas-flow Reynolds numbers at the rotor blades of approximately $1 \cdot 75$, $2 \cdot 0$ and $2 \cdot 5 \times 10^5$, at various incidences on to the rotor blades (*i.e.*, at various rotational speeds).

The clearance space was then closed with plasticine and a repeat efficiency calibration carried out.

2.3. *Rotor-Blade Cooling Characteristics at Higher Temperature Ratios.* Ref. 2 gives a comprehensive account of the cooling performance of the rotor blades at a turbine inlet gas temperature of 650 deg C to 700 deg C with a cooling-air inlet temperature of 80 deg C to 100 deg C. As the ratio T_g/T_{cr} increases, so also will the ratio of gas temperature to mean blade temperature (T_g/T_b) increase, together with the ratio of mean blade temperature to cooling-air temperature (T_b/T_{cr}). Now the external heat-transfer coefficient, at a given Reynolds number, may increase slightly with an increase in the ratio T_g/T_b and similarly it is known that a reduction in the internal heat-transfer coefficient occurs with increase in T_b/T_{cr} (Ref. 4). Therefore, it may be anticipated that an increase in the ratio of gas to cooling-air temperature will cause a small increase in the mean blade relative temperature (*i.e.*, a reduction in the relative degree of cooling) at a fixed value of cooling-flow ratio.

In order to confirm this, the turbine inlet gas temperature was increased in increments of approximately 100 deg C, maintaining the rotor-blade cooling-air temperature at 80 deg C to 100 deg C. The cooling-air flow ratio was varied at each increment, measurements of the rotor-blade metal temperatures being taken at each cooling-flow ratio.

2.4. *Endurance Tests at High Temperature.* In order to examine the operating characteristics and mechanical reliability, the turbine was operated for a period of 50 hours at a mean inlet gas temperature of 1400 deg K. The speed was maintained at 8000 r.p.m. which gave a mean gas incidence on to the rotor blades of about 4 deg at a Reynolds number of $0 \cdot 7 \times 10^5$. Throughout the tests the design values of cooling-air flows, given in Section 2.1, were applied except for the nozzle blades, where a flow of $2 \cdot 5$ per cent of the main gas-stream flow was applied. This was to prevent overheating of a few of the nozzle blades which were situated in regions of very high local gas temperature.

3. *Discussion of Results.* 3.1. *The Effect of Cooling-Air Discharge into the Main Gas Stream.* The effect of discharging cooling air from the inlet liners and the nozzle and rotor blades is illustrated in Fig. 2, where the turbine isentropic efficiency is plotted against stage work done coefficient for each individual cooling air discharge.

It is important to define carefully the manner in which efficiency is calculated, since widely different results may be obtained according to the manner in which efficiency is defined. Efficiency is generally defined as the ratio:

$$\frac{\left[\text{Work temperature drop over stage}\right]}{\left[\begin{array}{l}\text{Isentropic temperature drop over stage for same}\\ \text{total pressure ratio and turbine inlet temperature}\end{array}\right]} .$$

In the present tests, the work temperature drop (ΔT_w °C) is calculated from measurements of brake (or shaft) horsepower and gas mass-flow rate (W lb/sec).

Then

$$\Delta T_w\ (°\mathrm{C}) = \frac{H.P. \times 550}{J \times C_p \times W} .$$

It is at once apparent that different values of ΔT_w (and hence efficiency) can be obtained, depending upon whether or not the cooling flows through the liners and blades are regarded as part of the 'working' mass flow, W.

In the present calculations of efficiency, the cooling air discharged from the inlet liners and nozzle blades (w_1, w_2, w_3 and w_N) have been included as part of the total working mass flow (W).

With this method of calculation, small losses in efficiency occur when cooling-air flows are injected and at the optimum points are as follows:

(*a*) Inner annulus liner and nozzle shroud .. .. 0·4 per cent

(*b*) Outer annulus liner .. .. 1·0 per cent

(*c*) Nozzle blades .. .. 0·5 per cent

(*d*) Rotor blades .. .. 0·75 per cent

(*e*) Combined effect of (*a*) to (*d*) .. .. 2·0 per cent .

If, however, only the entry mass flow to the turbine were taken as the operating flow (the cooling flow w_N from the nozzle blades being discounted as working fluid), then instead of a reduction of 0·5 per cent due to the nozzle-blade cooling flow being recorded, an increase in efficiency of $1\frac{1}{2}$ per cent would be deduced. It can be argued that this would arise through the nozzle-blade cooling air partially filling the clearance space and in effect causing a reduction in tip clearance, which as shown later, increases the turbine efficiency considerably.

In the case of the rotor blades, due to the fact that the cooling air is discharged from the blade tips with a tangential component of velocity equal to the blade tip speed, there is an inevitable 'pumping' loss, *i.e.*, some of the torque transmitted to the rotor by the main gas stream must be absorbed to give the 2 per cent rotor-blade cooling-air mass flow this tangential component of velocity. Now this 'pumping' work is calculable (*see* Appendix 1) and it may be argued that it should be allowed for in the efficiency estimate, particularly since the basic aerodynamic efficiency of the stage is being sought along with the losses or changes that cannot be calculated. The inclusion of this pumping loss in the efficiency estimate would cause a calculated loss of approximately 1·25 per cent, whereas the measured efficiency shows a loss of only 0·75 per cent, so that it may be said that the discharge of cooling air from the blade tips improves the aerodynamic efficiency by about $\frac{1}{2}$ per cent. This presumably results from the cooling air partially filling the clearance space and causing an 'effective' reduction in tip clearance, as with the nozzle blades.

It should be noted that the use of effusion cooled blades would not reduce the pumping work since the effusion velocities normal to the surfaces would be very small and the cooling air would still be discharged from the surface with an absolute tangential velocity substantially equal to the blade speed. The pumping loss might only be reduced by discharging the cooling air from a hole or slot in such a way that it has a tangential component of velocity (relative to the blade) opposite in direction to that of the rotor blade (*e.g.*, by discharging through a trailing-edge slot).

A further point of interest lies in the fact that the losses in efficiency recorded when the component cooling-air supplies are applied individually are not strictly additive when all cooling-air supplies are operated simultaneously. Thus, the sum of the individual losses listed above amount to approximately 2·7 per cent, whereas Fig. 2 shows that the total loss of efficiency when all cooling flows are applied is only 2 per cent.

3.2. *The Effect of Nozzle-Blade Tip Clearance.* The increase in efficiency obtained by reducing the nozzle-blade tip clearance to zero is clearly shown in Fig. 3 where the theoretical estimate of a gain of very nearly 5 per cent is confirmed at each gas operating Reynolds number. This fully emphasises the importance of having a fully shrouded nozzle-blade tip, such that not only would there be no loss in efficiency due to tip clearance but also the variations in efficiency due to cooling-air discharge may be largely avoided.

It is of interest at this point to estimate the variation in turbine efficiency with Reynolds number at different blade tip clearances and this is illustrated in Fig. 4. The curves are related to a datum measured efficiency of 75 per cent (allowing for measured losses due to cooling-air discharge) at a rotor-blade Reynolds number of 2×10^5, a stage work done coefficient of 4·5 and a gas inlet temperature of 35 deg C (such that the clearances may be taken as those measured with the turbine stationary). The value of efficiency at Reynolds numbers other than 2×10^5 may then be calculated from either of two proposed equations:

$$(a)\ 1 - \eta = (1 - \eta_m)\left(\frac{2 \times 10^5}{Re}\right)^{0 \cdot 2} \qquad \text{(Moody)}$$

or

$$(b)\quad \eta = 1 - \tfrac{1}{2}(1 - \eta_m)\left\{1 + \left(\frac{2 \times 10^5}{Re}\right)^{0 \cdot 2}\right\}, \qquad \text{(Ackeret)}$$

where η is the turbine efficiency at the Reynolds number (Re) required and η_m is the measured turbine efficiency at a Reynolds number of 2×10^5.

Experimental data on the influence of Reynolds number on turbine performance in the range $7 \times 10^4 < Re < 2 \times 10^5$ is scant; but available data generally shows a rate of change of efficiency with Re which lies within the rates of change defined by the above empirical equations.

For the case of zero nozzle-blade tip clearance, the increase at $Re = 2 \times 10^5$ from Fig. 3 was taken and the efficiency curves deduced again from the above equations. This assumed an unchanged rotor-blade tip clearance.

To obtain the further increase in efficiency due to zero clearance on both nozzle and rotor, the method of Ref. 3 was used with allowance made for cooling-air discharge.

Superimposed on the curves are some efficiency plots obtained from tests on the turbine at 1400 deg K gas inlet temperature with the same blade loading coefficient $(2K_p.\Delta T/U_m{}^2) \simeq 4 \cdot 5$. These indicate that some gain in efficiency has been obtained over the values anticipated from the cold flow tests by reductions in both nozzle and rotor-blade tip clearances, though it is not possible to allocate amounts to each except by approximate calculations from some measured metal temperatures. These latter suggest that the increase is derived mainly from a nozzle-tip clearance reduction with little change in the rotor blade tip clearance. This deduction is also broadly substantiated by the fact that the cooling-air pressure losses in the nozzle blades at high gas temperatures were higher than those anticipated by calculations based on earlier lower temperature experiments[2], this higher loss probably being associated with the reduced tip clearance which would result in a smaller 'escape' area for the discharged cooling air.

3.3. *Rotor-Blade Cooling Characteristics at Higher Temperature Ratios.* The variation of blade temperature with gas to cooling-air temperature ratio is shown in Fig. 5 for certain selected rotor-blade positions. The test results are plotted non-dimensionally as 'blade relative temperature', where the blade relative temperature is defined as

$$\frac{\text{Blade temperature} - \text{Inlet cooling-air temperature}}{\text{'Effective' gas temperature} - \text{Inlet cooling-air temperature}} .$$

Since previous tests had indicated that the highest metal temperatures were measured at the couples located near the blade leading edge, the selected thermo-couples were those near the leading edge situated at the root, mean diameter and tip of the blades, along with those at the centre and towards the trailing edge of the blades at the mean-diameter position. These latter thermo-couples gave the metal temperatures in the vicinity of the most highly stressed part of the blade.

It will be seen from Fig. 5 that there is a reduction in the cooling effectiveness of the blade as the ratio, effective gas temperature to inlet cooling-air temperature, increases, although this reduction is less pronounced at temperature ratios above $3 \cdot 0$. At 1400 deg K, the cooling effectiveness is approximately $5\frac{1}{2}$ per cent below that at 925 deg K.

Also shown are the temperature contours on the blade surface when the effective gas temperature is 1285 deg K, equivalent to a gas inlet temperature to the turbine of 1380 deg K. The cooling-air inlet temperature is 100 deg C and the cooling-flow ration $0 \cdot 02$, while the gas-flow Reynolds number is taken at $0 \cdot 7 \times 10^5$. It can be seen that the stress-carrying centre of the blade is maintained at a temperature less than 800 deg C, the hottest part of the blade being at the mean-diameter trailing edge of the blade and attaining a temperature between 900 deg C and 1000 deg C.

3.4. *Endurance Tests at* 1400 *deg K.* Operation of the turbine at the higher inlet gas temperatures presented no difficulty. The gas temperature was increased in stages of 100 deg C commencing at 930 deg C and tests of about two hours' duration were made at each level of temperature until 1130 deg C (approximately 1400 deg K) had been reached where more prolonged tests of up to five hours' duration were carried out. In all, a total of 74 hours' testing, sub-divided into the following periods, was completed without major incident:

At	1200°K	9 hours
At	1300°K	15 hours
At	1400°K	50 hours .

Throughout the foregoing test period the blades, in particular the rotor blades, were examined for signs of pronounced blade creep or imminent blade failure. The rotor-blade tip clearance was measured after each test and the blades visually examined for surface cracks (so far as was possible without dismantling the rig), but no excessive elongation was recorded and, although the rotor blades had been subjected to heavy machining tool pressures on the concave side during manufacture, causing a few cooling holes to break through the blade surface, no signs of cracking or further deterioration due to this or other causes was observed.

A typical example of the condition of the rotor blades after 50 hours at 1400 deg K gas temperature is shown in Fig. 6, where it can be seen that a small amount of thermal distortion has taken place and the blade tips have a slight permanent set in the direction of rotation. The nozzle blades have also distorted very slightly in a similar manner. Fig. 7 shows one nozzle blade in particular which has been situated at the centre of the hottest combustion-chamber outlet and has been subjected to a very high gas temperature in the mid-span region (approximately 1550 to 1600 deg K; *see* Refs. 1 and 2 for gas temperature distributions). In this case it can be seen that a small amount of scaling has taken place on the leading edge. All blades appeared to be in a sound condition and they were regarded as satisfactory for further high-temperature testing.

Following the first period of 25 hours at 1400 deg K some trouble was experienced with the rotor blade tip shroud, which is a stationary member machined integrally with the ring containing the cooled nozzle blades (*see* Fig. 1). It was appreciated that this shroud would be subjected to high thermal stresses as it would be in direct contact with the hot gas stream in the vicinity of the rotor-blade tips and in contact with incoming cooling air in the vicinity of the nozzle-blade roots. For this reason a number of axial slots were cut in the shroud to relieve these stresses. Unfortunately the slots were evidently subject to high local concentrations of stress at the ends of the slots and both cracking and distortion of the shroud ring occurred, the latter tending to reduce the rotor-blade tip clearance at some points to a dangerous level (*see* Fig. 8). Redesign of this section of the turbine, with the object of fitting a separate shroud ring of symmetrical cross-section which could expand freely, was found to be difficult without major modification to the turbine and a similar nozzle ring with integral rotor shroud but without slots was therefore fitted. The final period of 25 hours at 1400 deg K was completed without repetition of the trouble.

3.5. *Cooling-Air Pressure Loss.* (*a*) *Pressure loss in rotor-blade cooling passages with zero heat transfer.* The measured pressure drop of the cooling air passing through the rotor-blade cooling passages, expressed in the conventional non-dimensional terms, is shown in Fig. 9. Curves are presented of the mean of a number of unused blades and a number of turbine blades after a total of 250 hours' testing in the turbine (including 25 hours at 1400 deg K) and these are compared with values calculated assuming normal pipe friction coefficients for smooth pipe flow. These curves indicate that on an engine, where the cooling-air supply pressure would remain constant, a reduction in cooling-air flow of approximately 5 per cent (*i.e.*, about 0·1 per cent of main gas flow) would occur through the rotor blades in the higher cooling-flow range after similar prolonged running and would have almost negligible effect on the cooling effectiveness of the blades.

This small flow reduction at a fixed cooling pressure drop is most probably associated with a very fine deposit occurring on the walls of the cooling passages. A change in hole size was eliminated by travelling microscope measurements which did not show any appreciable discrepancy between unused and used blades. Now the pressure drop through such a cooling hole is approximately inversely proportional to d^5. Therefore if a deposit occurred on the walls of the cooling holes of 0·001 in. thickness, an increase in pressure drop of approximately 40 per cent would result for the same cooling mass flow. Fig. 9, however, shows that there was only about 10 per cent increase in pressure drop at the maximum cooling flow, indicating that any deposit that did occur within the cooling passages was less than 0·0005 in. thick. With cooling air flowing through the passages and the blade being at a much higher temperature, the cooling air on the passage surface would be at a higher temperature than that in the centre of passage. This would mean that the mean molecular velocities of the air near the passage surface, being higher than those in the main stream, would tend to drive small particles in the air stream towards the passage centre and, along with the centrifugal action from the rotating blade, would tend to allay any deposit on the cooling passage wall.

(*b*) *Losses in the rotor-blade cooling system.* Ref. 2 illustrated the effect on the rotor-blade cooling-air pressure-drop ratio of an increased gas temperature to cooling-air temperature ratio. The cooling-air pressure-drop ratio was defined as

$$(P_{cr} - \bar{p}_{sr})/(P_i - \bar{p}_{sr}),$$

where

P_{cr} = inlet total pressure of cooling air (measured in the present instance at the point where the rotor blade cooling air is fed into the hollow rotor shaft)

$\bar{p}_{sr}$ = mean static pressure at the rotor blade tip

P_i = total pressure of gas flow at inlet to the turbine.

If this ratio is greater than approximately $1 \cdot 05$ to $1 \cdot 1$, compression of the cooling air, above that of the compressor delivery, would be required to force the cooling air through the rotor-blade cooling passages. As the ratio of inlet gas temperature to cooling-air inlet temperature increases, this pressure-drop ratio decreases. Thus, for a given air pressure drop across the blade cooling passages a greater proportion of cooling air will be passed at increased temperature ratios.

This effect is clearly shown in Fig. 10 which is an extension of Fig. 25 in Ref. 2. At the highest temperature ratio ($T_g/T_{cr} = 3 \cdot 5$) and turbine speed (8000 r.p.m.) so far reached, it would be possible with the present disc and blade arrangement, to attain a cooling-flow ratio of $0 \cdot 019$ before the cooling-air pressure required exceeded the turbine inlet total pressure. It must be added that whereas the curves of Ref. 2 were for a gas-flow Reynolds number of 1×10^5, the final temperature-ratio curve in Fig. 10 is for a Reynolds number of $0 \cdot 7 \times 10^5$. It may therefore be expected that at the higher-value Reynolds number the cooling-flow ratio obtainable would be further slightly increased due to the resultant increase in cooling-air Reynolds number and a reduction in the friction coefficient.

(*c*) *Losses in the nozzle-blade cooling system.* For the nozzle blades, the cooling-air pressure drop is expressed non-dimensionally as:

$$(P_{cn} - \bar{p}_{sn})/(P_i - \bar{p}_{sn})$$

where

P_{cn} = inlet total pressure of cooling air measured in the annular header surrounding the nozzle root fixing

$\bar{p}_{sn}$ = mean static pressure at nozzle blade tip

P_i = turbine gas inlet total pressure.

Contrary to the rotor blades, the effect of increasing the gas to cooling-air temperature ratio was shown in Ref. 2, to increase the cooling-air pressure-drop ratio. This was attributed to the differential expansion of the nozzle-blade clamping ring, the nozzle blades and the shroud ring at the nozzle blade tips. Fig. 10b, however, indicates that at the highest temperature ratio so far reached, there is in fact a small reduction in the cooling-air pressure-drop ratio in the higher cooling-flow range (above about $0 \cdot 02$). In this Figure, the gas-flow Reynolds number at the nozzle blades for the highest temperature ratio was 2×10^5, whilst those at the lower temperature ratios were 4×10^5. Some reduction in pressure-loss ratio may therefore be anticipated for the highest temperature ratio with the increased Reynolds number. This change in trend may be attributed to a small variation in the expansion of the nozzle-blade tip shroud at higher gas temperatures, probably caused by variations in the temperature distribution at outlet from the combustion chambers at the increased burner pressures.

4. *Conclusions.* Further experiments have been carried out on a high temperature air-cooled turbine to determine the effects of:

(*a*) cooling-air discharge into the main gas stream

(*b*) nozzle-blade tip clearance

(*c*) rotor-blade cooling characteristics at higher ratios of gas temperature to cooling-air inlet temperature

(*d*) operation of the turbine at an inlet gas temperature of 1400 deg K.

The following conclusions may be drawn from these experiments:

1. Discharge of cooling air into the main gas stream created variations in the turbine-stage aerodynamic efficiency probably due to the disturbance of the main-gas-stream boundary layer. Where the cooling-air flow from the nozzle blades is considered to be part of the main working gas flow passing through the rotor row to produce external work, then the design values of cooling-air flows create the following reductions in efficiency:

(i) Inner annulus liner and nozzle shroud cooling air	0·4 per cent
(ii) Outer annulus liner cooling air	1·0 per cent
(iii) Nozzle-blade cooling air	0·5 per cent
(iv) Rotor-blade cooling air	0·75 per cent
(v) Combined effect of (i) to (iv)	2·0 per cent

If the nozzle-blade cooling air is not considered to be part of the working gas stream, then item (iii) proves to be beneficial and creates an increase in efficiency of 1·5 per cent, presumably by the cooling air effectively reducing the nozzle-blade tip clearance.
In the case of the rotor blades, the 'pumping' loss (*i.e.*, the power taken from the turbine blades to eject the cooling air with a component of velocity in the direction of rotation) is calculated at 1·25 per cent, whereas the measured efficiency reduction is only 0·75 per cent and may be attributed to the cooling air again effectively reducing the rotor-blade tip clearance.

2. Elimination of the nozzle-blade tip clearance increased the turbine efficiency by 5 per cent. This clearly emphasises the desirability of a fully shrouded nozzle blade tip.

3. An increase in the turbine inlet gas temperature to 1400 deg K whilst maintaining the cooling-air inlet temperature constant reduced the cooling effectiveness of the rotor blades by approximately 5 per cent below that recorded in earlier tests at 1000 deg K. This is due to a reduction in the internal heat-transfer coefficient (as the ratio mean blade temperature

to cooling-air inlet temperature increases), possibly combined with an increase in the external heat-transfer coefficient (as the ratio gas temperature to mean blade temperature increases).

4. Operation of the turbine at a mean gas inlet temperature of 1400 deg K was achieved without difficulty for a period of 50 hours, although a small structural failure in the rotor-blade shroud ring occurred after 25 hours of this period. Slight modifications to this were necessary before further testing could be carried out and proved successful. A small amount of distortion and scaling occurred on both rotor and nozzle blades, but insufficient to prevent them being used in further high temperature testing.
5. The cooling-air pressure loss in the rotor blade showed no significant change in trend at the higher temperature ratios from the results at lower values of gas inlet temperature. The losses are such that at the highest temperature ratio so far achieved a rotor cooling-flow ratio of approximately 0·019 could be achieved in the present design of turbine and blade with a maximum cooling-air pressure equal to the compressor delivery pressure.
6. In the case of the nozzle blades, a small change in trend occurred in the pressure-drop ratio at the higher cooling flows and higher turbine inlet gas temperatures. This is probably due to the changes in temperature distribution at the higher burner pressures producing variations in the metal temperature distribution and ultimately in nozzle-blade tip clearance. The maximum cooling-flow ratio obtainable with the cooling-air pressure equal to the compressor delivery pressure at the highest temperature ratio so far achieved is approximately 0·018 in the present system.

NOTATION

K_p	Absolute specific heat of gas at constant pressure (foot poundal/lb/°C)
C_p	Normal specific heat of gas at constant pressure (C.H.U./lb/°C)
J	Mechanical equivalent of heat
$\bar{p}_{sn}$	Mean static pressure at nozzle blade tip
$\bar{p}_{sr}$	Mean static pressure at rotor blade tip
P_i	Total pressure of gas flow at inlet to turbine
P_{cn}	Total pressure of nozzle cooling air at entry
P_{cr}	Total pressure of rotor cooling air at entry
Re	Gas-flow Reynolds number based on blade chord, outlet velocity relative to the blade and density and viscosity based on gas static temperature and pressure at blade outlet
U_m	Mean-diameter rotor-blade speed
w_N	Cooling-air mass flow to nozzle row
w_R	Cooling-air mass flow to rotor row
w_1	Cooling-air mass flow to outer liner
w_2	Cooling-air mass flow to inner liner
w_3	Cooling-air mass flow to nozzle-blade tip shroud
W_r	Gas mass flow through rotor row
ΔT_w	Gas total temperature drop through stage corresponding to the stage work output to drive shaft
η	Turbine isentropic expansion efficiency
η_m	Turbine isentropic expansion efficiency at $Re = 2 \times 10^5$
U_{tip}	Rotor-blade tip speed
r_{tip}	Rotor-blade tip radius
N	Turbine rotational speed
T_g^*	'Effective' gas temperature
T_i	Turbine gas inlet temperature
T_{cr}	Cooling-air temperature at blade root
T_b	Blade local metal temperature
A_h	Area of cooling-hole passages in rotor blade
d	Diameter of one cooling-hole passage.

REFERENCES

No.	Author	Title, etc.
1	D. G. Ainley and N. E. Waldren ..	Investigations on an experimental air-cooled turbine. Part I.—General description of turbine and experimental technique. R. & M. 2975. March, 1954.
2	D. G. Ainley, N. E. Waldren and K. Hughes	Investigations on an experimental air-cooled turbine. Part II.—Cooling characteristics of blades having a multiplicity of small diameter coolant passages. R. & M. 2975. March, 1954.
3	D. G. Ainley and G. C. R. Mathieson ..	A method of performance estimation for axial-flow turbines. R. & M. 2974. December, 1951.
4	L. V. Humble, W. H. Lowdermilk and L. G. Desmon	Measurements of average heat-transfer and friction coefficients for subsonic flow of air in smooth tubes at high surface and fluid temperatures. N.A.C.A. Report 1020. 1951.

APPENDIX I

Rotor-Blade Pumping Losses

$$\Delta T_w = \frac{\text{Brake torque} \times 2\pi N}{C_p J (W + w_1 + w_2 + w_3 + w_N)}$$

$$\eta = \frac{\Delta T_w}{\Delta T(\text{isen})}.$$

Torque produced by main gas stream

$$= (\text{Brake torque}) + (\text{pumping torque})$$

where 'pumping torque' is the torque required to spill 2 per cent of the main gas flow from rotor blade tips with tangential component of velocity of U_{tip}

Therefore

$$\text{pumping torque} = 0\cdot 02(W + w_1 + w_2 + w_3 + w_N) \times \frac{U_{\text{tip}} \times r_{\text{tip}}}{g}$$

Therefore

$$\Delta T\ (\text{blade work}) = \frac{\text{Total torque} \times 2\pi N}{C_p J(W + w_1 + w_2 + w_3 + w_N)}$$

$$= \frac{(\text{Brake torque} + \text{pumping torque}) \times 2\pi N}{C_p J(W + w_1 + w_2 + w_3 + w_N)}$$

$$= \frac{\left[\dfrac{\Delta T_w C_p J(W + w_1 + w_2 + w_3 + w_N)}{2\pi N} + \dfrac{0\cdot 02(W + w_1 + w_2 + w_3 + w_N) U_{\text{tip}}\, r_{\text{tip}} \times 2\pi N}{g}\right]}{C_p J(W + w_1 + w_2 + w_3 + w_N)}$$

$$= \Delta T_w + \frac{0\cdot 02\ U_{\text{tip}}\, r_{\text{tip}}}{g J C_p} \frac{U_{\text{tip}}}{r_{\text{tip}}}$$

$$= \Delta T_w \left[1 + \frac{0\cdot 02 \times 2}{\dfrac{2K_p \Delta T_w}{U_{\text{tip}}^2}}\right]$$

$$= \Delta T_w \left[1 + \left(\frac{0\cdot 04}{\dfrac{2K_p \Delta T_w}{U_m^2}}\right) \frac{U_{\text{tip}}^2}{U_m^2}\right].$$

Thus when

$$2K_p . \Delta T_w / U_m^2 = 4\cdot 0\,,$$

$$\Delta T\ \text{blade work} = \Delta T_w \times 1\cdot 0125.$$

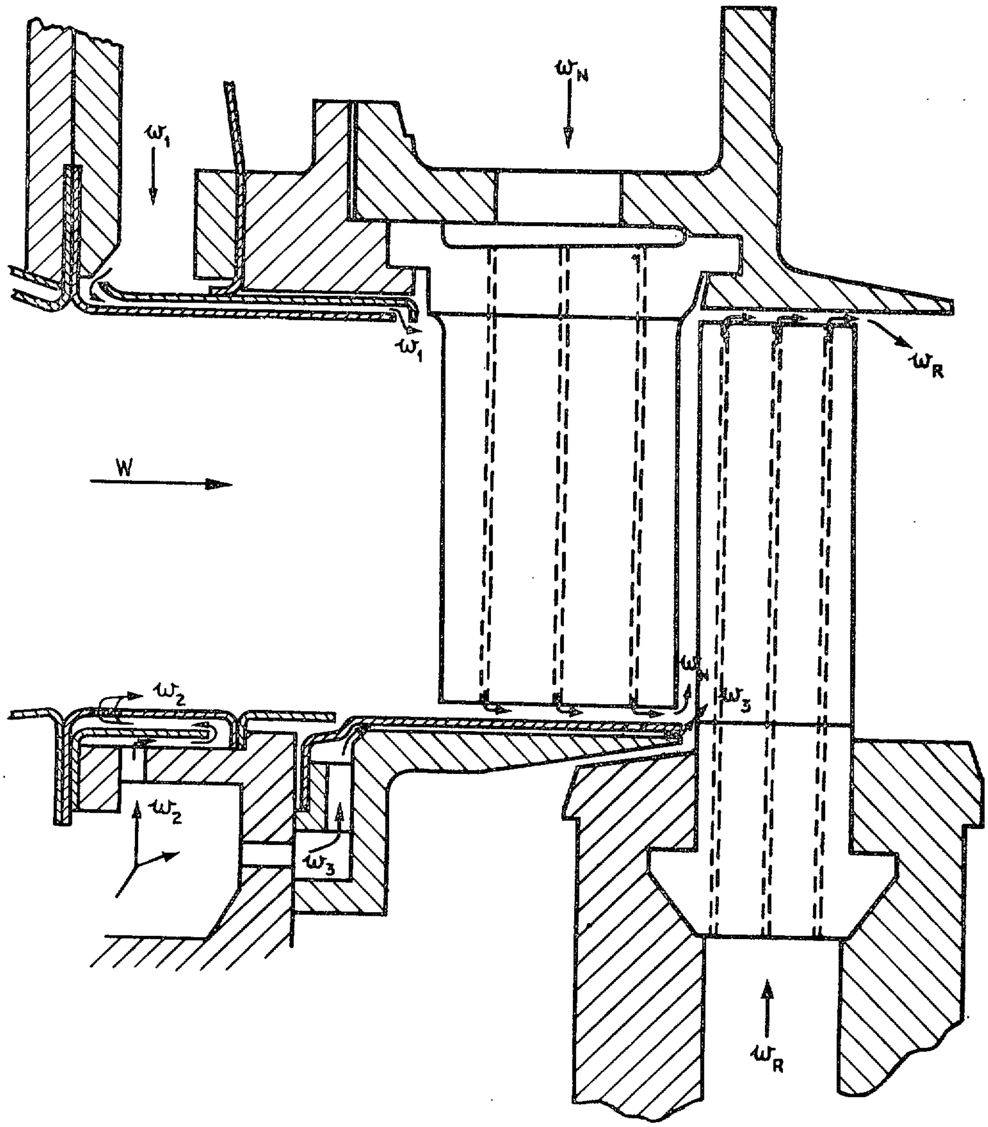

Fig. 1. Cooling-air flow through turbine stage.

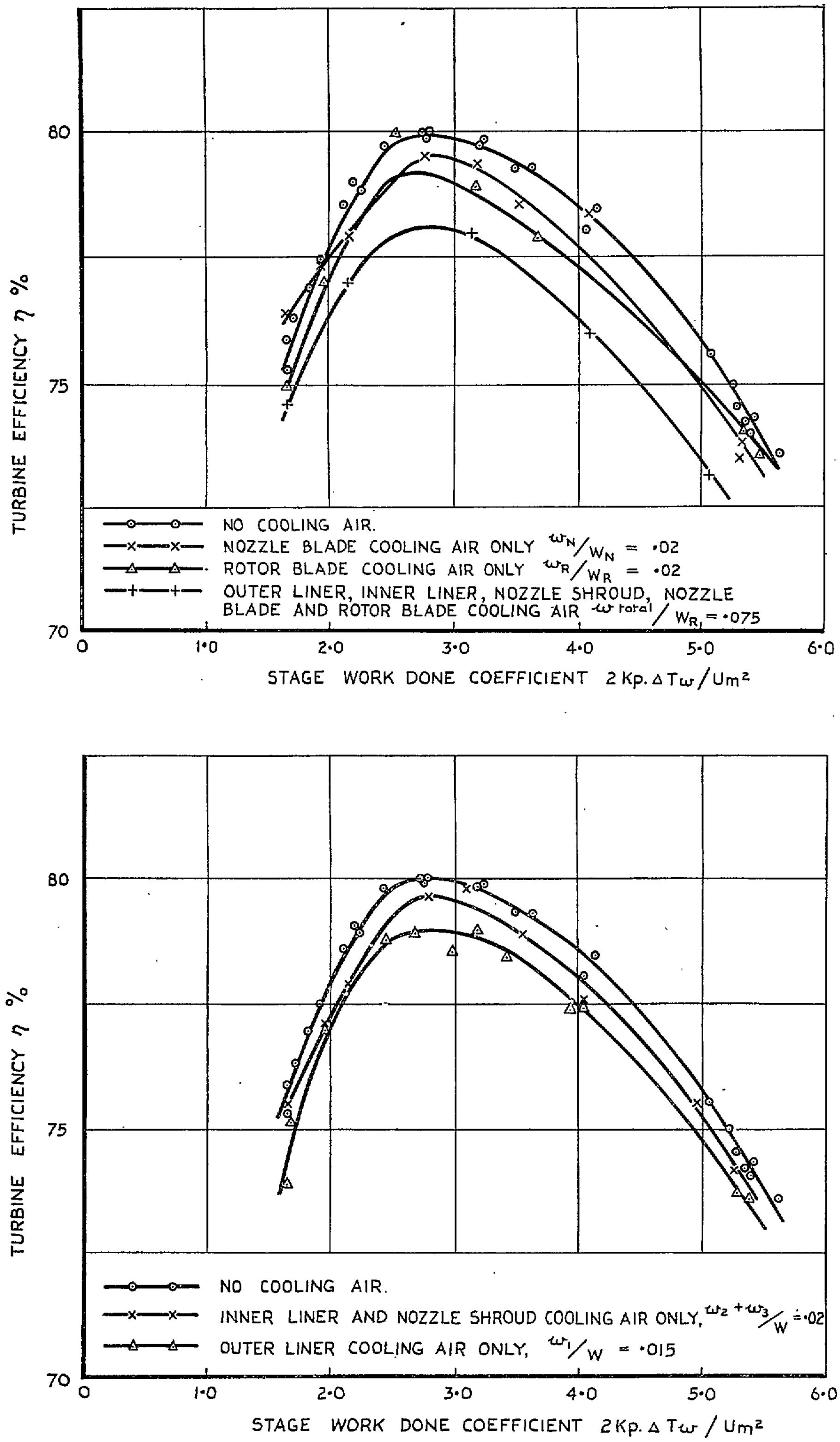

FIG. 2. Effect on turbine aerodynamic efficiency of discharge of cooling air ($Re = 2 \times 10^5$).

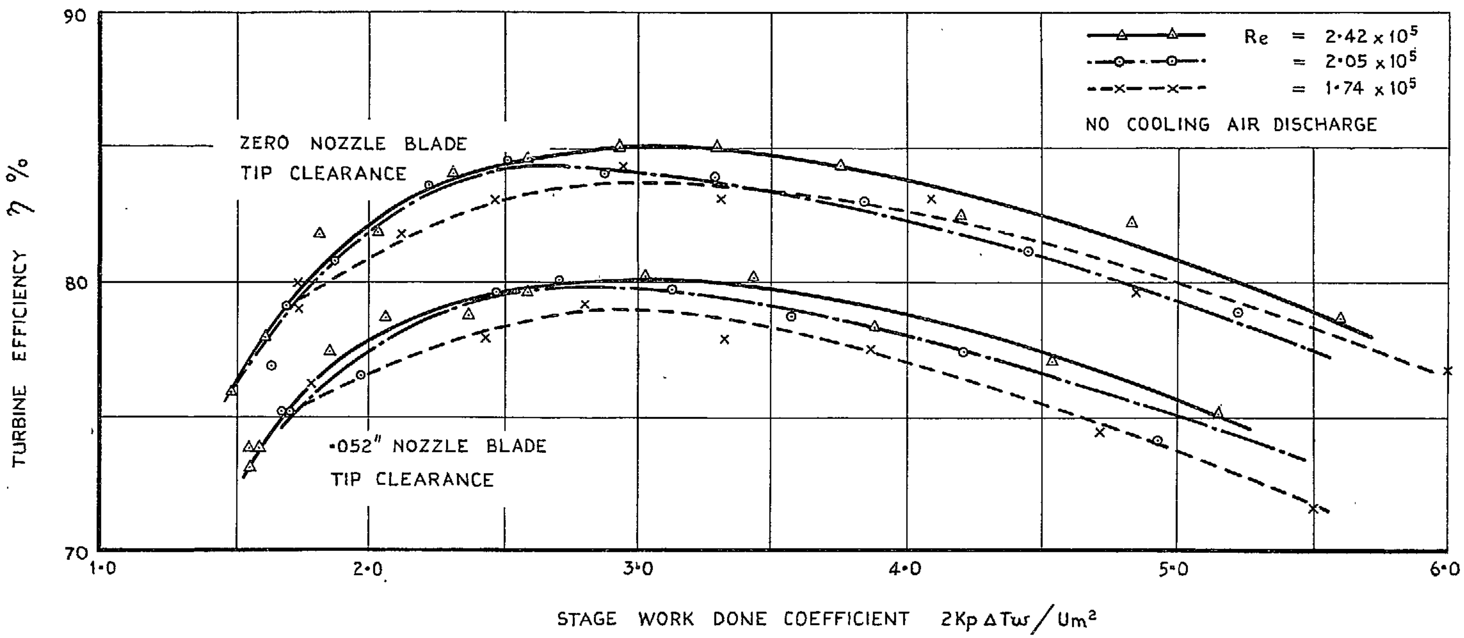

FIG. 3. Effect of nozzle-blade tip clearance on aerodynamic efficiency.

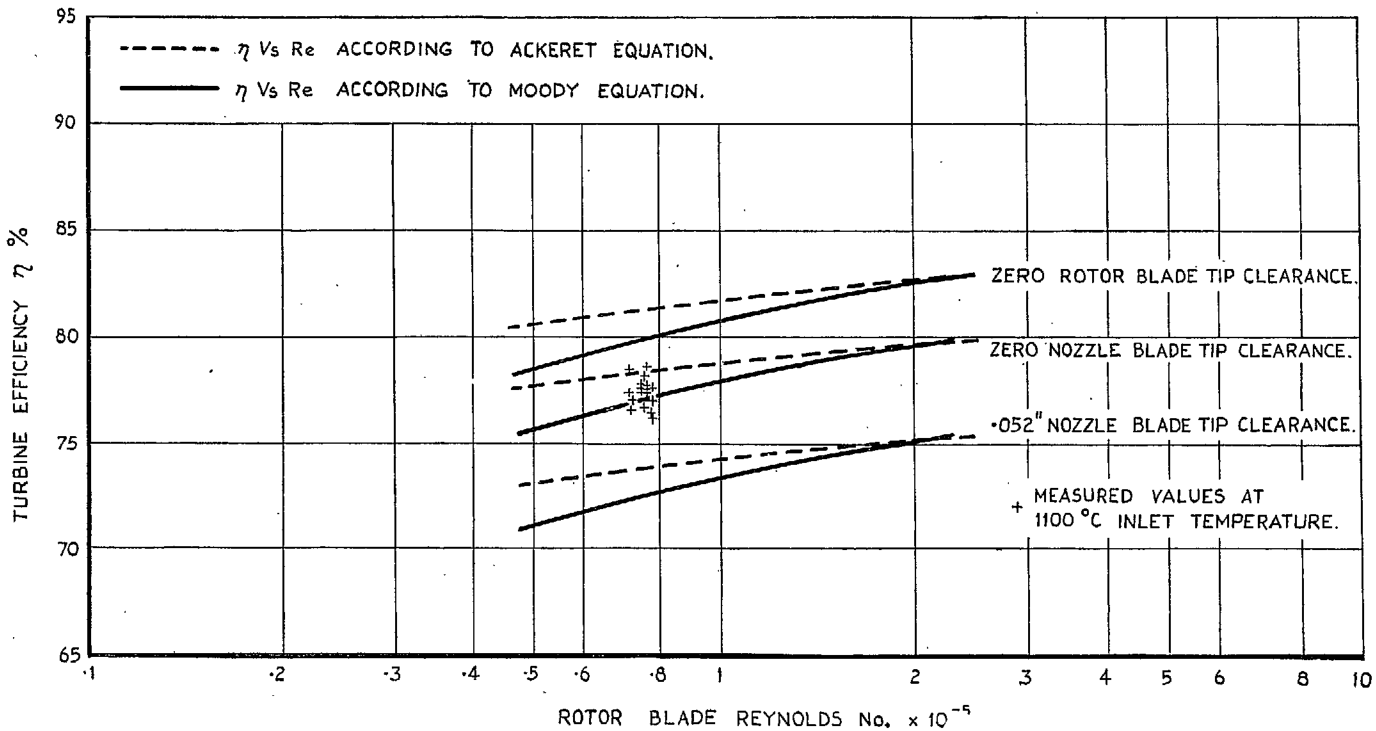

FIG. 4. Variation of turbine aerodynamic efficiency with Reynolds number ($2K_p.\Delta T_w/U_m^2 = 4\cdot5$; allowance made for losses due to cooling-air discharge).

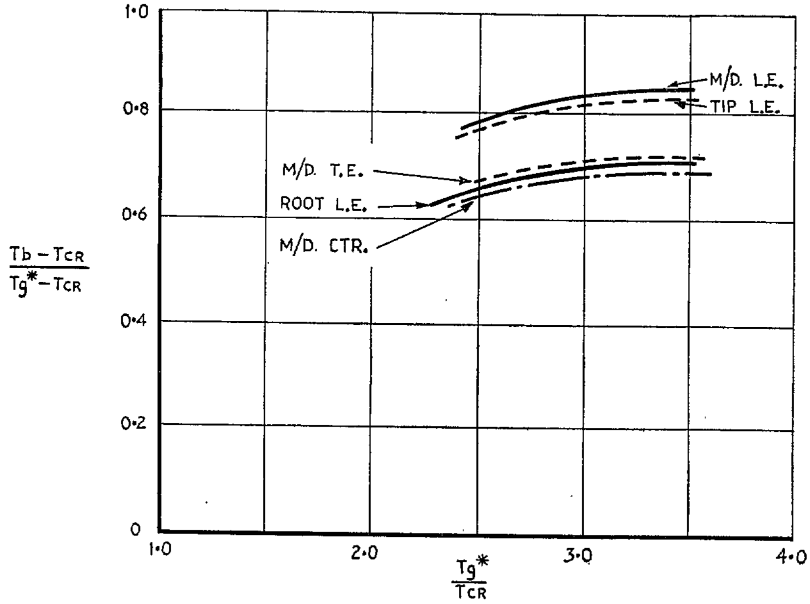

EFFECT OF GAS TO COOLING AIR TEMPERATURE RATIO ON COOLING CHARACTERISTIC OF BLADE.

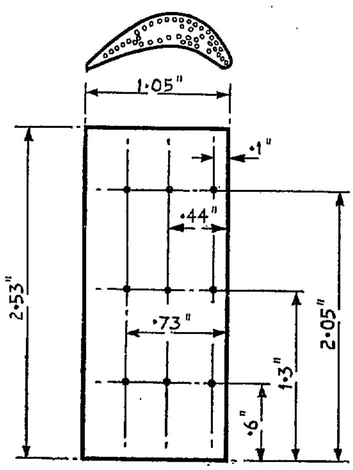

LOCATION OF THERMOCOUPLES IN ROTOR BLADE.

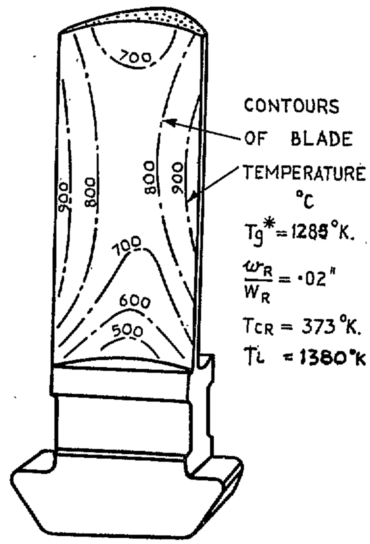

ROTOR BLADE METAL TEMPERATURE CONTOURS.

Fig. 5. Cooling characteristics of rotor blade at higher gas temperatures.

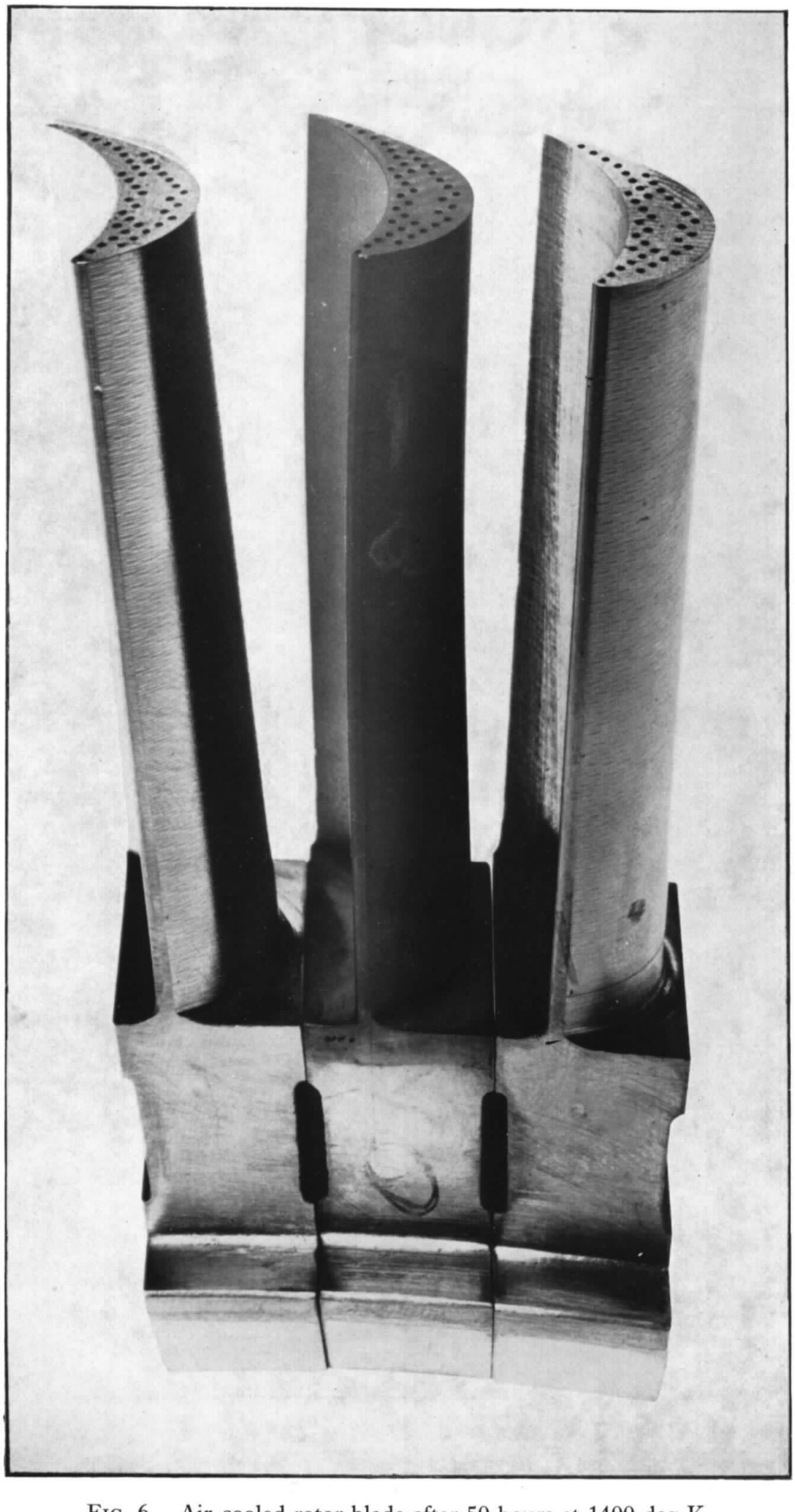

FIG. 6. Air-cooled rotor blade after 50 hours at 1400 deg K.

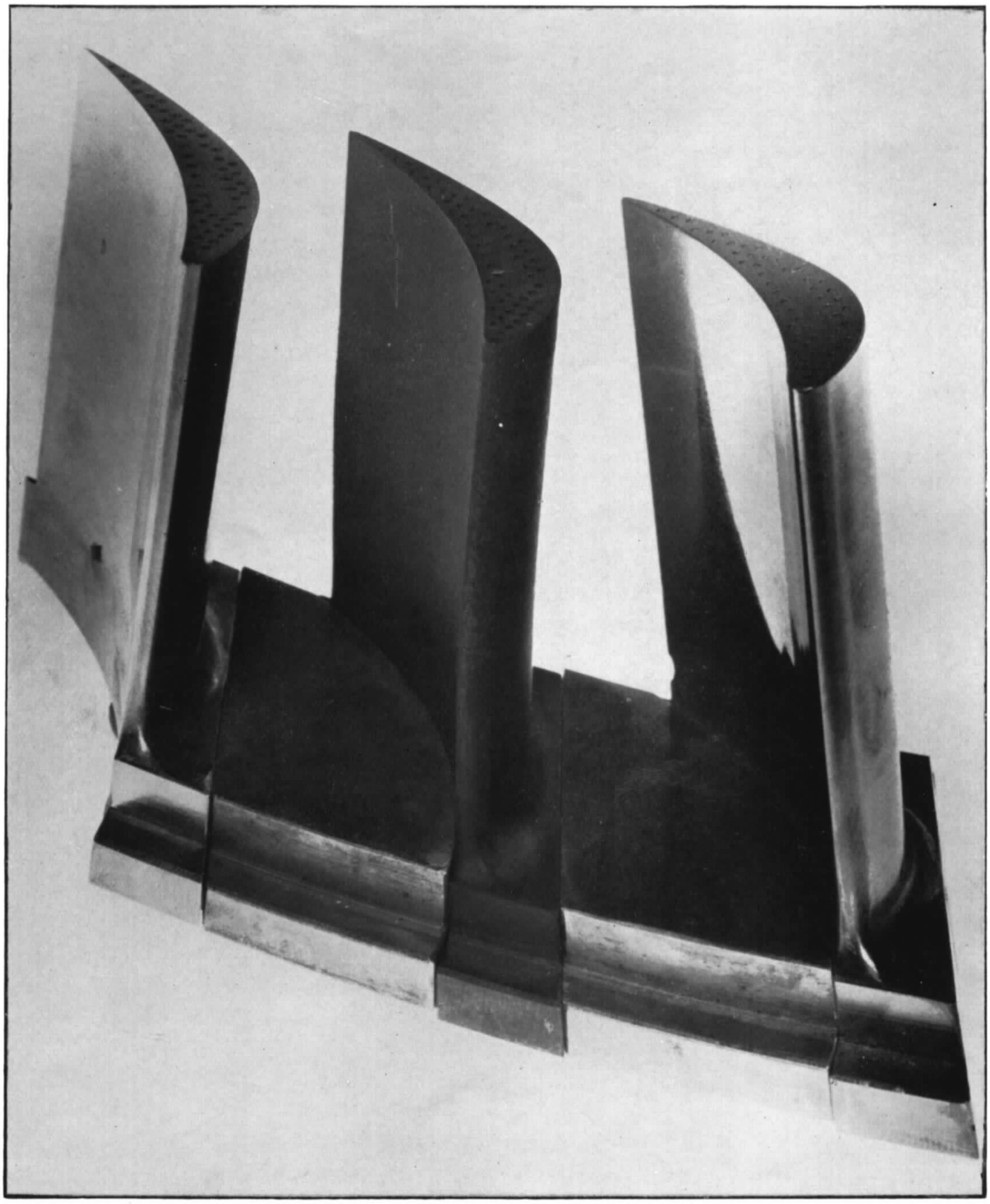

FIG. 7. Air-cooled nozzle blade after 50 hours at 1400 deg K.

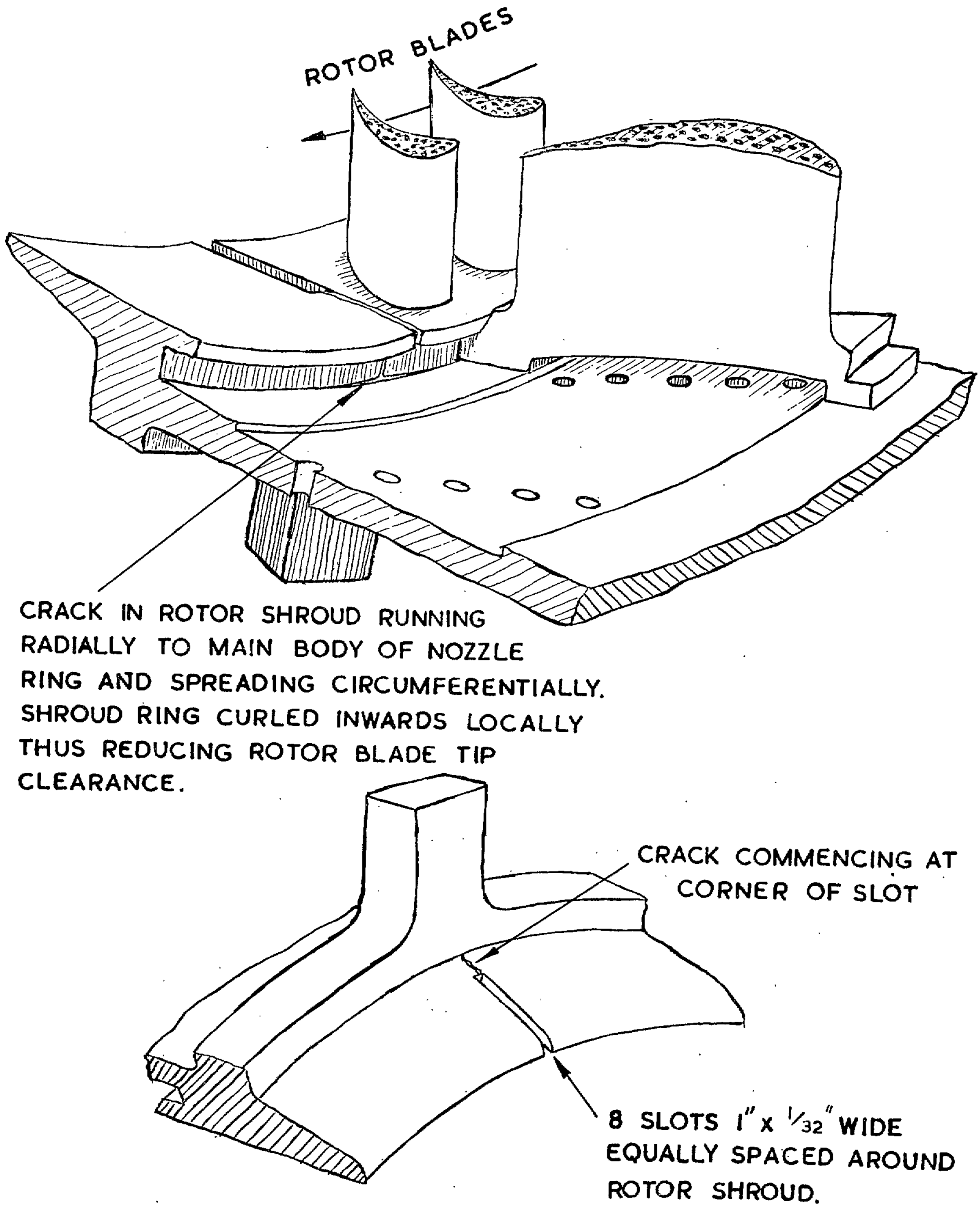

FIG. 8. Failure in rotor shroud ring.

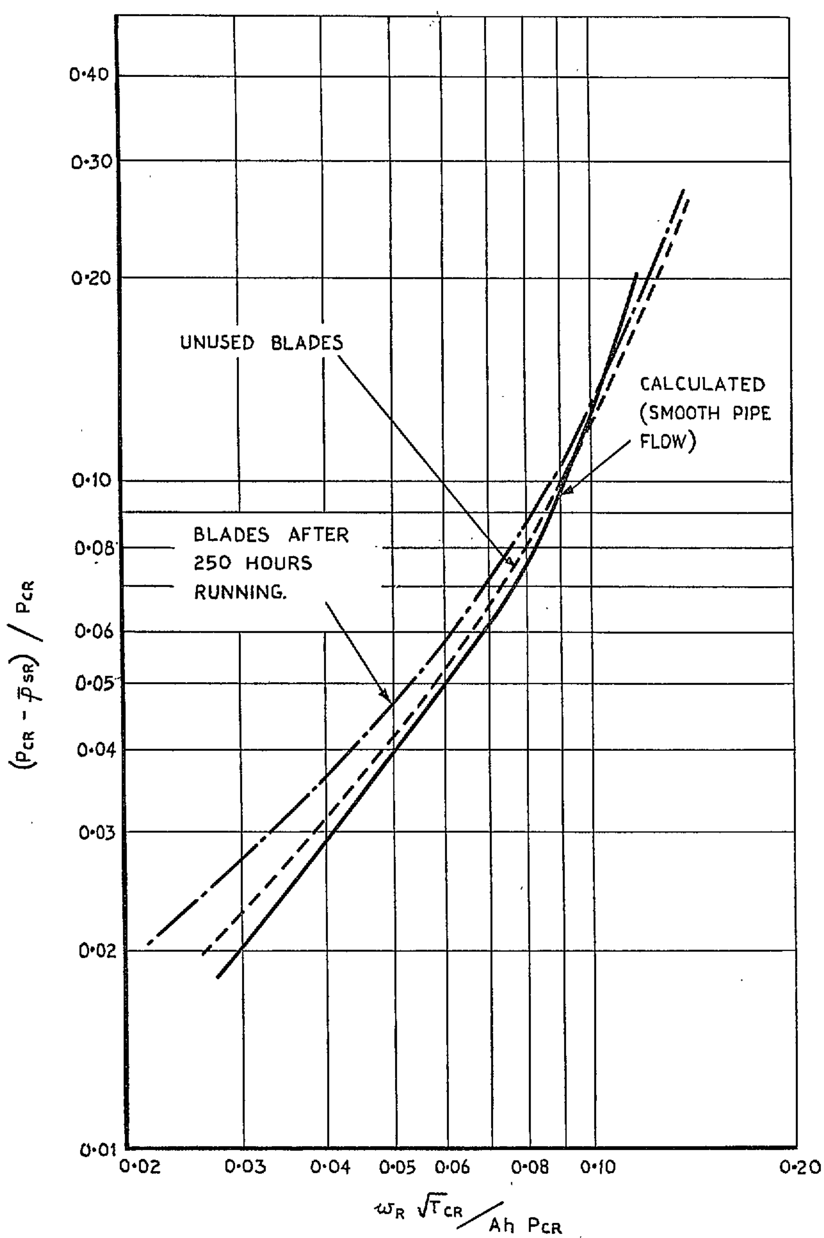

$\bar{p}_{SR}$ = STATIC PRESSURE AT BLADE TIP.

T_{CI} = COOLING AIR TEMPERATURE.

P_{CR} = TOTAL PRESSURE OF COOLING AIR ENTERING BLADE ROOT.

w_R = COOLING AIR MASS FLOW TO BLADE.

Ah = TOTAL CROSS SECTIONAL AREA OF BLADE COOLING PASSAGES.

FIG. 9. Pressure losses in rotor-blade cooling-air passages (No heat transfer).

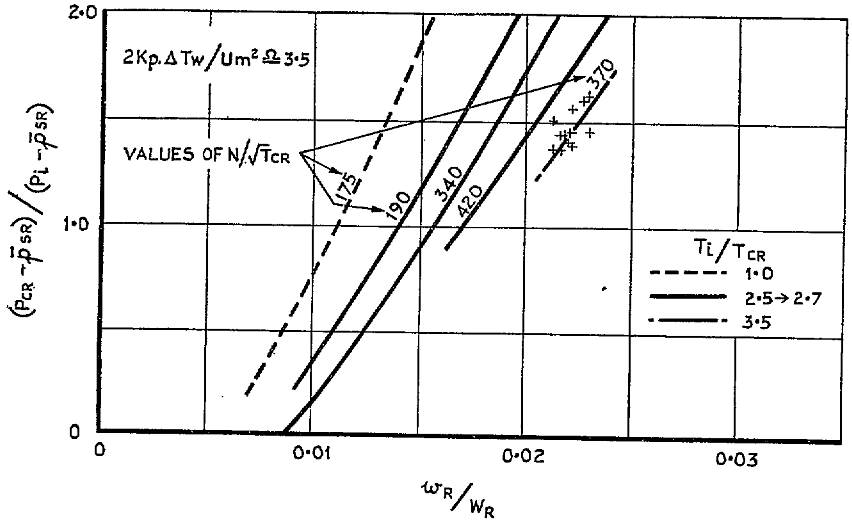

(a) ROTOR ROW.

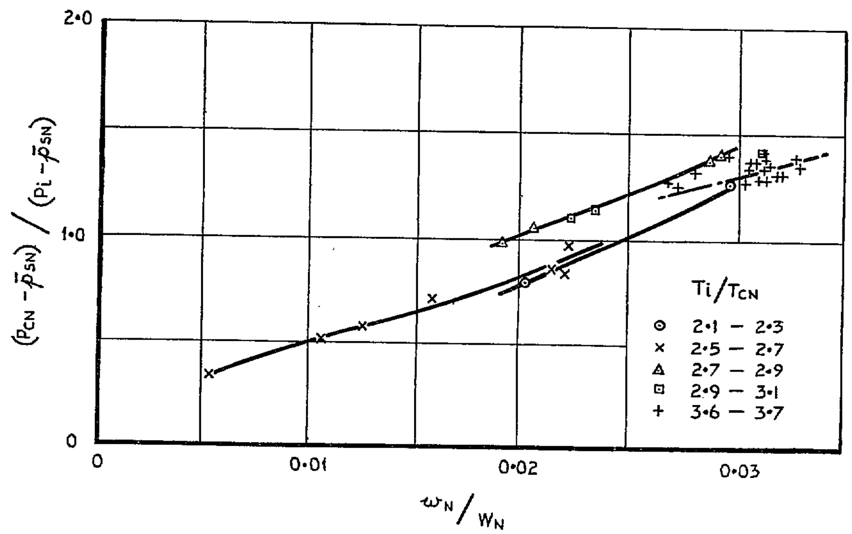

(b) NOZZLE ROW.

Figs. 10a and 10b. Variation of cooling-air pressure drop with cooling-air quantity.

(78656)

Part IV.—Examination of Sintered Vitallium Air-Cooled Turbine Blades Following 100 Hours' Operation at a Turbine Inlet Mean Gas Temperature of 1400 deg K

By N. E. WALDREN and C. J. HART

Summary. A set of sintered vitallium air-cooled nozzle and rotor blades has been examined following a period of 100 hours' operation with a turbine inlet mean gas temperature of 1400 deg K. The blades, in particular the rotor blades, have distorted in a manner contrary to that which had been generally expected and cracks have formed in the sharp trailing edges and internally, around cooling passages in the region of the leading edge.

Turbine tests and tests carried out in the laboratory suggest that the cracks in the trailing edges of the blades are due primarily to the repeated high thermal stresses set up by non-uniform heating and cooling, and the unexpected distortion in the rotor blades is the result of creep strain under a combination of steady thermal and centrifugal stresses. The distortion in the nozzle blades is associated with combined thermal and gas bending stresses.

In the rotor blades internal cracking has been caused by excessive tensile creep strain in local regions in the blade, associated with the blade distortion, and it is possible that cooling passages in the vicinity have accelerated failure. Chordwise cracking in the blade trailing edges is accentuated by their razor-like form and their consequent weakness to thermal fatigue or thermal shock is to be expected.

Fortunately, other factors which may influence future trends in cooled blade design result in a blade shape which is less susceptible to the distortion and cracking as exhibited by the present sintered vitallium blades. In principle these are (i) more rounded and slightly thicker trailing edges and (ii) no more than moderate degrees of blade camber.

---

1. *Introduction.* The experimental single-stage air-cooled turbine and test rig have already been described in detail[1], and the cooling performance of the sintered vitallium blades has been thoroughly analysed[2]. It is now proposed to examine the mechanical behaviour of the air-cooled blades and the effects resulting from operation at high gas temperatures over a total period of 268 hours, the latter 100 hours being at a turbine inlet mean gas temperature of 1400 deg K.

Throughout the period of test running the blades, in particular the rotor blades, were kept under close observation for signs of cracking, excessive elongation or distortion. As testing at 1400 deg K progressed the rotor blades began to show particularly a marked distortion in a manner contrary to that which had been generally expected. Testing at the high temperature was continued to observe further growth of this phenomenon but was finally terminated when cracks began to appear in both the nozzle and rotor-blade trailing edges.

Distortion and cracking in the blading may be due to a number of reasons, namely, thermal shock, thermal fatigue, vibration fatigue, local creep strains or some changes in metal structure occurring locally due to prolonged exposure to high temperature. It is proposed, therefore, to study the material properties, estimated stresses and measured distortion in the blades together with laboratory tests on individual blades, with a view to isolating the main cause or causes of the incipient blade failure.

2. *Blade Manufacture and Material Properties.* The vitallium nozzle and rotor blades are shown in Figs. 1 and 2 and relevant dimensions are tabulated in Appendix I.

The method of manufacture has been described before in Ref. 4, but, briefly, the blades were formed by powder metallurgy, the cooling holes being produced by inserting cadmium wire cores into the powder. After compressing the powder, heat treatment at 650 deg C vaporised the cadmium wire cores and sintering at 1325 deg C for 8 hours produced billets containing cooling passages from which the blades were subsequently machined.

At the time of manufacture difficulty was experienced in maintaining the requisite amount of carbon normally present in the original casting version of vitallium alloy. Lower (negligible) carbon content resulted in a more ductile blade material with a resistance to creep much lower than anticipated. However, the mechanical properties were acceptable for the proposed tests and these properties, together with the composition of the final blade material are given in Figs. 5 and 16, and Appendix II.

Due to lack of machining experience on this type of blade relatively heavy cuts were taken on the concave surface when finishing the rotor blades, causing partial collapse of the metal in the vicinity of some cooling passages. This left the concave surface of the final rotor blades with a certain degree of work hardening in the material. This trouble was avoided when machining the convex surface of the rotor blades and the complete nozzle blades.

3. *Turbine Operating Conditions.* A large portion of the initial testing on the turbine was carried out at moderate gas temperatures less than 900 deg C with the prime object of obtaining blade-cooling and heat-transfer data (*see* Fig. 6). Cooling air to the blades was varied over a wide range and blade temperature ranged from a mean of approximately 500 deg C up to gas temperature. Following this period of testing, gas temperature was progressively increased, cooling air again being varied but limited by a rotor-blade mean temperature of approximately 820 deg C, until the turbine was eventually operating at a mean gas inlet temperature of 1127 deg C (1400 deg K). Following the first 50-hour period at this gas temperature the turbine was dismantled and it was noticed that both nozzle and rotor blades showed signs of distortion. At this stage, one nozzle blade and six randomly selected rotor blades were removed to examine for possible internal cracks due to the presence of cooling passages and all seven blades were replaced by new spares.

Testing continued, tests varying from 1 to 5 hours in duration, until a total of 100 hours at a gas-stream temperature of 1400 deg K had been completed. During this latter period the distortion which was by now becoming quite noticeable, was measured in both the new and a number of the original rotor blades after each 5 hours of testing. The results are plotted in Fig. 7 and indicate that there is a marked relation between rotor-blade distortion and testing time. At the end of the 100-hours period of testing at 1400 deg K small cracks had become apparent in the rotor-blade trailing edges and a small piece from the tip of one nozzle-blade trailing edge had broken away and caused slight damage to five further nozzle-blade trailing edges (Fig. 3).

Although the turbine casing was originally designed to permit operation at an inlet gas temperature up to 1200 deg C it was found that the maldistribution in turbine inlet temperature as delivered by the eight combustion chambers[1, 2], imposed a severe limitation on the maximum operating temperature. Nozzle blades situated directly opposite the centre of each combustion-chamber outlet were subjected to very high local gas temperatures during the final 100 hours' testing and gas temperature traverses[1] gave indication that this local gas temperature exceeded 1300 deg C. When combined with cooling-air starvation in the blade leading edges due to non-uniform coolant flow (caused by the static pressure gradient at the unshrouded blade tips (*see* Ref. 2)), these high local gas temperatures resulted in very high metal temperatures at some nozzle-blade leading edges. This, coupled with the further difficulty of measuring temperature at this high level, made a precise estimation of the conditions experienced by the nozzle blades extremely difficult.

In the case of the rotor blades, the problem of estimating local conditions was eased to some degree as the blades experienced only a mean circumferential gas temperature at each spanwise position due to their high rotational speed, the gas temperature which would most severely limit turbine operation being that occurring at approximately mid-stream, *i.e.*, relative to the rotor blade at mid-height. During the last 100 hours' testing this mid-stream gas temperature relative to the rotor row was approximately 1100 deg C.

The power output from the single-stage turbine and consequently the gas loading on the blading was relatively low in comparison with the design maximum. During the final 100 hours' period of testing the power was approximately 950 h.p. at a rotational speed of 7500 to 8000 r.p.m. (9000 r.p.m. design)*.

At the beginning and end of each test gas temperature was varied slowly to avoid substantial thermal shock to the blades, and when testing at 1400 deg K the gas temperature cycle was roughly as shown in Fig. 6. Between the initial heat-transfer tests and the final endurance running, however, a number of deliberate and strong thermal shock tests were made when the fuel was suddenly cut and the gas temperature dropped from a mean of 990 deg C to the pre-combustion air temperature (120 deg C). A total of five shocks were made at the time with no apparent ill-effect on the blades.

4. *Examination of Turbine Blades.* A typical example of the distortion which has taken place in the rotor blades following tests in the turbine is shown in Fig. 1. The blade is noticeably bent about the mid-span region, the root and tip portions, however, remaining quite straight. In general the surface appearance of the blades confirms the measured temperature distribution shown in Fig. 1. Both the oxide film and, in particular, the very slight amount of scaling indicate that the highest temperatures have occurred in the mid-span region of the leading and trailing edges, the region about which the blades have distorted.

From a random selection of five blades careful dimensional checks confirm that the bend has taken place about a neutral axis passing approximately through the trailing edge and lying at roughly 30 deg to the blade chord (Figs. 8 and 9). At the neutral axis no measurable extension on the original blade length has taken place. Towards the leading edges, however, the extension progressively increases to between 0·02 to 0·04 in. It is probable that the greater part of this extension occurs locally in the distorted portion of the blade span (*see* Fig. 8). In the trailing edges slight buckling has also occurred and small chordwise cracks have formed. In all, thirty-five of the ninety-nine rotor blades had trailing-edge cracks and, of the six new rotor blades fitted, four are included in this number. It is interesting to note that in blades exhibiting maximum distortion, no trailing-edge cracks were observed.

A surface examination of the blades after the initial 50 hours' operation at 1400 deg K together with the examination of a sectioned blade removed at this stage, gave no clear indication of cracking

* Rig operation was restricted to a maximum rotational speed of approximately 8000 r.p.m. due to the onset of a spasmodic but sharply defined increase in general rig vibration at higher speeds.

either externally or internally. At the end of the 100-hour period at 1400 deg K, however, in addition to the trailing-edge cracks already mentioned, the examination of three sectioned blades showed cracking around a number of the cooling passages near the leading edge in the mid-span region (Fig. 4).

The three blades selected for sectioning were No. 119 which had a pronounced distortion only, No. 108 which showed both distortion and trailing-edge cracking, and No. 144, a replacement blade, which had been subjected only to the final 50 hours at 1400 deg K and showed a small amount of distortion together with trailing-edge cracks. The mid-span portion of each blade was sectioned through the leading edge normal to the axis of distortion and sections include cooling passages as shown in Fig. 4.

In general, cracks appear to be intergranular and have initiated from the cooling passages, spreading in the worst cases, through cavities representing 1 per cent to 2 per cent porosity or through alumina particles in the sintered material. The majority of the cracks occur in a region midway between the leading edge and the neutral axis of distortion. Either side of this region the material appears to be free from cracking, although some changes in metal structure are apparent in the extreme leading-edge region. In blade No. 119 cracks approximately 0·015 in. in length have formed (*see* Fig. 4) but in blades Nos. 108 and 144 in which less distortion has taken place, internal cracking is much less severe, the worse cracks being approximately 0·002 in. in length.

Under the microscope the external surface around the blade leading edges and adjacent to the internal cracks shows an oxide layer of moderate proportions with a small amount of erosion, but no cracking in the surface could be seen using non-destructive crack-detection methods.

In the nozzle blades, apart from the slight damage to a limited number of trailing edges caused by the breakaway of the trailing edge of blade No. 10 shown in Fig. 3, cracking has been limited to the trailing edges of two other blades, one having very slight signs of cracking similar to blade No. 10 and the remaining blade No. 39 having a large chordwise crack in the trailing edge at approximately blade mid-height, shown in Fig. 2. All cracked blades were situated opposite the centre of combustion chamber outlets and thermo-couples positioned at mid-height in blade No. 39 indicated a temperature of almost 900 deg C at the trailing edge (Fig. 10). The leading edges of all nozzle blades showed signs of erosion, the amount being greater at mid-height and on blades which had been situated directly opposite a combustion-chamber outlet. Maximum leading-edge temperature on these blades is uncertain, but very probably exceeds 1000 deg C. In the worst case, however, this erosion is not considered severe and, in general, the majority of the forty-five blades are in sound condition.

Examining blade No. 10 in more detail, the failure has taken the form of cracks through the extreme trailing-edge cooling passage in a spanwise direction. These cracks isolated a strip of trailing edge approximately $\frac{1}{4}$ in. wide and $\frac{7}{8}$ in. long. About $\frac{1}{2}$ in. of the tip has broken away and the remaining portion has curled to a greater degree than the adjacent part of the blade.

The distortion that has occurred in the nozzle blades is shown in Figs. 2 and 10. Without exception the blades have bent at the root and curled back in the opposite sense towards the tip, the distortion being more pronounced in those blades which have been subjected to the hottest part of the gas stream. The bending at the root has taken place about an axis parallel to the blade chord. Towards the tip, however, this axis rotates slightly giving a small twist to the blade.

5. *Discussion of Rotor-Blade Failure.* Under turbine operating conditions stress in the cooled blades is produced by the combined effect of a number of causes. These might be listed as:

(i) Centrifugal force, resulting in centrifugal stress which decreases roughly linearly from a high value at the root of the blade span to zero at the tip.

(ii) Non-uniform temperature, resulting in non-uniform expansion of the blade material and hence thermal stress. A steady state of non-uniformity in temperature will arise due to non-uniformity in cooling during steady running of the turbine, the degree of non-uniformity varying with the selected operating condition of the turbine. A further transient non-uniformity in temperature will arise during starting and stopping of the turbine, although this may be minimised by changing conditions slowly.

(iii) Gas loading, resulting in gas bending stresses which decrease rapidly from the root towards the tip.

(iv) Blade variation, resulting in alternating bending stresses which may vary spanwise in various ways depending on the particular mode of vibration.

The mechanical behaviour exhibited by the blades will be controlled by the resultant effect of all these factors, although it is probable that only one or two may be of dominant influence. It is therefore of interest to speculate upon the influence that each of these individual factors might exert.

5.1. *Influence of Centrifugal Stress.* Fig. 13b shows the variation of stress over the blade span due to centrifugal force. This stress, when related to the mean blade temperature at each spanwise position, indicates that the weakest part of the blade lies in the mid-span region and, as this coincides roughly with the region where maximum distortion has actually occurred in the blade, it would seem that centrifugal stress has had some significant influence on the blade distortion.

5.2. *Influence of Thermal Stress.* An estimate of the thermal stress due to non-uniform cooling across the blade chord at the weakest point in the span is shown in Fig. 14. The calculation has assumed that the blade is free to expand and bend but no yield has taken place in the material[2]. From this Figure it can be seen that thermal stress at the hot leading and trailing edges is of a sufficiently high level to cause local yield in compression. On cooling to a uniform low temperature therefore, high tensile stresses will occur in the regions where compressive yield has taken place and the blade will tend to distort in an opposite manner to that in Fig. 1 and cracks may form in the leading and trailing edges.

In seeking confirmation of the foregoing theory and to further study the effect of a non-uniform chordwise temperature distribution on a cooled turbine blade, tests were carried out in the laboratory on separate, new rotor blades with cooling passages. A non-uniform chordwise temperature distribution similar to that in the turbine (*see* Fig. 14a), was reproduced in the blades by heating at the mid-span region with an oxy-acetylene flame and passing cooling air through the passages.

Two aspects of the problem were examined. Firstly, a blade was subjected to a prolonged period under the foregoing conditions with the object of allowing creep strain under thermal stress alone to take place while, at the same time, avoiding any tendency to thermal shock the blade by rapid heating or cooling. A total of 50 hours was completed in $2\frac{1}{2}$ to 3-hour periods.

Secondly, a blade was subjected to 100 thermal cycles between a cooling-air temperature of 20 deg C and the required chordwise temperature maldistribution, 5 minutes being allowed for heating, 5 minutes for soaking and 5 minutes for cooling. This represented moderate turbine starting and shut-down conditions, *i.e.*, a mild form of thermal shock.

The results of these tests are summarized in Fig. 12. In each case distortion took place about the heated mid-span region but, as previously suggested, in an opposite sense to that in the turbine and trailing edge chordwise cracks formed at an early stage. It can therefore be concluded that:

(i) Although the level of thermal stress in the blades is of a magnitude which will cause local yield and distortion, this thermal stress alone does not cause the distortion as exhibited by the blades in the turbine.

(ii) The formation of cracks in the blade trailing edges is almost certainly associated with thermal cycling and, although not necessarily due to thermal shock, this may accentuate the tendency to crack.

5.3. *Influence of Blade Vibration.* The substantial rotor-blade section of thickness/chord ratio $= 0\cdot234$, the position of the axis of the bend (30 deg to the axis of minimum stiffness), together with a bending fatigue factor of between 5 and 6 for 10^7 cycles at 900 deg C[2], would suggest that vibration stresses are unlikely to have any significant influence in this analysis. However, in an effort to confirm this view, further tests were carried out in the laboratory in continuation of those in the previous Section 5.2. A third blade was subjected as before to a chordwise temperature maldistribution, then excited at the tip until a 'natural' frequency ranging from 200 to 280 c.p.s. at an amplitude of $\pm 0\cdot010$ in. to $\pm 0\cdot012$ in. was obtained. A total of 20 hours was completed in 3 to $3\frac{1}{2}$-hour periods. The frequency obtained was much lower than that which would be expected in the turbine, being due to the unavoidable additional mass of the vibrator, but nevertheless, it was thought that these tests would serve to indicate any effects due to alternating stress.

The results of the tests are summarized in Fig. 12. Once again trailing-edge cracks formed at an early stage and as these were more severe than in the previous two test blades, it would suggest that the superimposed alternating stress has accentuated the tendency to cracking in the relatively sharp trailing edges. The distortion that has occurred, does not substantially differ from that due to thermal stress alone and, therefore, does not explain the distortion that has taken place in the turbine blades.

5.4. *Influence of Gas Bending Stress.* Gas bending stress may ultimately cause creep in the blade, leading to distortion of the type observed in the turbine if centrifugal force is present. However, gas loading during the turbine tests was relatively low due to a low turbine power output and, at the weak mid-span region, about which distortion has taken place, the effect of gas loading is considerably reduced as shown in Fig. 13a. Further, the opposing moment produced by centrifugal force which tends to restore the distorted blade to its original shape is far greater than the moment due to gas loading. The effect of gas bending stress can therefore be disregarded in this discussion.

5.5. *Influence of Combined Centrifugal and Thermal Stresses.* The calculation of thermal stress discussed in Section 5.2 has assumed no temperature variation normal to the blade chord. The camber in the blade, however, has produced a variation in thermal stress between the upper and lower surfaces of the blade and a relatively high tensile stress on the blade lower surface in the mid-chord region results.

When centrifugal stress is superimposed on the blade thermal-stress pattern the result can be seen in Fig. 15. Both the tensile stress and the effective area over which the stress is tensile in the mid-chord region have been increased and the maximum stress on the lower surface has reached a value where yield can occur. Conversely, the compressive stress in the leading and trailing edges has been reduced with a corresponding reduction in the effective area of compression. Depending on the magnitude of the centrifugal stress, therefore, non-uniform yield across the blade in the mid-chord region can cause bending in the manner shown in Fig. 1. On cooling to a uniform low temperature and on removal of the centrifugal stress, the larger mid-chord section which was previously distorted under tension will restrain the leading and trailing edges and high tensile stresses in these latter regions will result.

Referring to Fig. 15 in more detail, the addition of 3 tons/sq in. centrifugal stress (value at 55 per cent of the span from the blade root) has increased the stress level near the blade lower surface in the mid-chord region to a value where a relatively large amount of creep strain in 100 hours will occur in the material. The progressive nature of the distortion in the blade as plotted in Fig. 7 would suggest that secondary creep has taken place and the analysis of the blade distortion after 100 hours' operation at 1400 deg K (Fig. 9) indicates that at least 1 per cent strain has actually taken place locally on the concave side at the mid-chord region.

In Fig. 14a actual thermo-couple readings at a gas temperature of 1400 deg K indicate a higher level of blade temperature than the chordwise temperature distribution extrapolated from low temperature tests from which thermal stress has been calculated. In Ref. 3 this difference has been shown to be due to the effect of the increase in the ratio of gas to cooling-air temperature and its main influence on this analysis has been to bring the region of high tensile stress nearer towards the leading edge than estimated in Figs. 14 and 15. This is shown approximately in Fig. 15 in which curves of creep strain based on actual thermo-couple readings are plotted, although no adjustment has been made to the curves of thermal stress which would further influence the trend.

In the leading and trailing edges the compressive stresses due to non-uniform cooling have been reduced by the addition of centrifugal stress but still remain at a level where large compressive creep strains can occur during operation, or as suggested in Ref. 2, could cause buckling (as in the narrow trailing edges), thus tending to reduce their influence on the thermal stress level in that region.

Referring to Fig. 15, therefore, large tensile creep strains towards the under-surface in the leading-edge region coupled with structural weakness in the trailing edge have caused the rotor blades to distort about an axis lying approximately 30 deg to the axis of minimum stiffness of the blade.

Internal cracking as described in Section 4 has been shown to be more severe around cooling passages in the leading-edge region, increasing in size with increase in blade distortion. From a further study of Fig. 15, this cracking can be attributed to excessive tensile creep strain in this region and, as some cracks originate from cooling holes, it would seem that the presence of holes in the blade has made some small contribution to the failure. In addition to the probable stress concentration produced by holes in the blade, cracking from the holes would be accentuated by the fact that metal temperature will decrease locally in the vicinity of each hole, leading to further increases in tensile stress in the metal forming the cooling-hole surface.

In the leading and trailing edges the amount of tensile strain on turbine 'shut down' will depend on the compressive creep strain in each region together with the general distortion in the blade over the period of each individual test. In the leading edges extensions of between 0·020 in. and 0·040 in. were measured after the 100-hour total operation at 1400 deg K and as the majority of this extension has undoubtedly occurred in the distorted mid-span region a strain of 4 per cent or more may have taken place locally in the leading edge of those blades exhibiting excessive distortion, similar to blade No. 119. The absence of cracking at the extreme leading edges under these conditions of stress reversal and excessive tensile yield must be attributed to the relatively high ductility of the material.

In the trailing edges where the general distortion in the blade has had little influence, the buckling combined with the stress concentration around the razor-like edges has made this region susceptible to failure under conditions similar to those experienced by the leading edges. In consequence, a number of blades exhibited chordwise cracks and, as noted in Section 4, these have occurred in blades showing only a moderate amount of distortion and would confirm a wide scatter in material properties.

5.6. *Conclusions on Rotor-Blade Failure.* Summarizing the previous Sections, it has been shown that:

(i) Distortion in the turbine rotor blades has been due, primarily, to the combined influence of centrifugal force and a non-uniform chordwise blade temperature, non-uniform tensile creep strain in the blade mid-span resulting. Excessive distortion has led to local tensile creep cracking which has most probably been aggravated by the presence of cooling holes.

(ii) Chordwise cracking in the rotor-blade trailing edges has been due to high tensile stress in this region on turbine 'shut down' following compressive yield during turbine operation, a number of cycles being necessary to cause failure. This type of cracking has been accentuated by the razor-like form of the trailing edge and, as demonstrated by laboratory tests, can be aggravated by blade vibration.

Both distortion and cracking can therefore be largely attributed to the non-uniform chordwise blade temperature and could undoubtedly be alleviated to a considerable degree by more uniform blade cooling. It would appear, however, that distortion might be further alleviated by reducing the blade camber, from which the stress gradient normal to the blade chord originates. (This can be demonstrated in Fig. 15 in which the stress level on the lower surface near the mid-chord would tend towards the mean value indicated by the dotted line as the blade camber is reduced.) It is possible that trends in turbine design associated with blade cooling may result in blades having relatively low camber, this feature being dictated by the need for economic use of cooling air and consequently for minimising the blade surface area in a cooled blade row. One method of achieving this is to design turbine stages with a higher ratio of axial gas velocity to blade peripheral speed, resulting in reduced blade camber and gas outlet angle.

In addition to improvements which could be obtained by more uniform blade cooling, chordwise cracking in the rotor-blade trailing edges might be further alleviated by increasing the trailing-edge thickness. A more substantial, rounded trailing edge would avoid, to some extent, the high local stress that can occur in a narrow trailing edge together with the tendency to buckle and aggravate distortion in the blades. A thicker trailing edge would have the additional advantage of permitting more cooling passages to be accommodated in this region, with resulting improvement in chordwise temperature distribution.

In Ref. 2 the operational life of the rotor blades at the higher gas temperatures was discussed and an estimate of the probable life of the rotor blades was made, using data obtained from tests at moderate gas temperatures. It was appreciated that a number of factors of obscure significance might substantially modify any estimate on blade life that was attempted. It is therefore difficult to draw a direct comparison between the life suggested in Ref. 2 and the actual results achieved from operating for 100 hours at a turbine inlet gas temperature of 1400 deg K. However, at least two points which have had a significant bearing on the life of the rotor blades have become more apparent from the high temperature tests. Firstly, a wide variation in material creep properties between blades has been indicated by the varying amounts of distortion that have taken place. Only a small number of rotor blades, *i.e.*, approximately 15 per cent, have actually exhibited the excessive distortion which has led to internal creep cracking. Secondly, and more important, is the increase in the ratio of gas to cooling-air temperature which has modified the blade chordwise temperature distribution shown in Fig. 14a and resulted in an increase in blade metal temperature over that which had been predicted at the weak mid-span, mid-chord region. This increase from an original estimate of 675 deg C to the 735 deg C actually measured can account for a considerable reduction in rotor-blade life as shown by the stress-to-rupture data plotted in Fig. 16 and in general, would confirm the 100 hours' life suggested by the onset of creep cracking.

Unfortunately, due to the complex stress problem introduced by the cooled rotor blades together with the limited amount of relevant data to hand, it is not possible to discuss the blades in more than general terms. The conclusions reached in this discussion are therefore of a qualitative nature only and it is quite possible that further research into the various aspects of blade cooling may modify them to some degree.

6. *Discussion on Nozzle-Blade Failure.* Due to the difficulty of estimating thermal stress in the nozzle blades it is proposed to make only a brief study of the distortion and cracking, in the light of the foregoing analysis of the rotor-blade failure.

In comparison with the rotor blades the camber in the nozzle blades is much lower and consequently the gradient of thermal stress between upper and lower surfaces of the nozzle blades will be less severe than in the rotor blades. However, the nozzle blades were operating at a much higher level of metal temperature and the effect of even a small additional stress on the blade lower surface could result in bending similar to the rotor blades.

Fig. 10 indicates the manner in which the nozzle blades have distorted. At the blade root where gas bending stress is greatest (*see* Fig. 13a,) the blades have bent in a similar direction to the rotor blades but, in this case, bending has taken place about the axis of minimum stiffness as would normally be expected under gas loading. Towards the blade tip, where gas loading is very small, the blades have curled in the opposite direction. Again, this would be expected from the results of laboratory tests on rotor blades in which thermal forces alone were significant.

The chordwise crack that has occurred in the trailing edge of blade No. 39 shown in Fig. 2 can be attributed to the same causes as for those in the rotor-blade trailing edges, *i.e.*, high tensile stress on turbine 'shut down'. This is the only nozzle blade in which a crack of this nature has appeared and it seems probable that failure was accelerated by its position in the turbine, being directly opposite the centre of a combustion-chamber outlet. In addition to thermo-couple readings a high blade temperature is confirmed by the relative severity of leading-edge erosion and the magnitude of the bend. Unlike the rotor blades, however, bending in the nozzle blades about an axis parallel to the chord could aggravate cracking in the trailing edge and may be the reason for the relatively large crack that has formed.

Spanwise cracks which have formed on either side of the trailing-edge cooling passage in nozzle blade No. 10 have also appeared in one other blade, but to a lesser degree. The cracks have originated at the tip of the trailing-edge upper surface where the condition of the blade surface indicates a high metal temperature. In both blades the extreme trailing-edge cooling passage was situated close to the upper surface whereas in the remaining forty-three blades this cooling passage was nearer the lower surface. This may have had some influence on the failure. Again both blades were situated directly opposite the centre of combustion chamber outlets, clear of turbulent wakes produced by the joints between adjacent combustion chambers, and cascade results[2] would suggest a condition of flow around the blades which would result in a higher input of heat to the upper surface than to the lower surface of the trailing edge. This could produce more severe conditions of thermal stress on the upper surface resulting in thermal fatigue about an axis approximately parallel to the cooling passages and, combined with a local weakness due to the position of the cooling passage, could be the cause of failure.

7. *Conclusions.* A set of air-cooled sintered vitallium nozzle and rotor blades has been examined following 100 hours' operation at a turbine inlet gas temperature of 1400 deg K and the possible causes of the distortion and cracking which have appeared in the blades have been reviewed. It has been shown that:

(1) Distortion in the cooled blades has been caused primarily by the thermal stress pattern resulting from non-uniform chordwise cooling. This pattern produces a high level of compressive stress in the leading and trailing edges and, in conjunction with the blade camber, it also produces a gradient of tensile stress normal to the blade chord in the mid-chord region.

(2) Additional stress, due to centrifugal loading in the rotor blades and gas loading in the nozzle blades, when superimposed on the thermal-stress gradient normal to the blade chord has reversed the direction of distortion due to thermal stress alone by reducing the compressive stress at the leading and trailing edges and increasing the tensile stress at the mid-chord region to a level at which large creep strains have occurred on the under surface. Weakness in the blade, *i.e.*, in the thin rotor-blade trailing edges, has led to local buckling with a consequent modification to the major distortion.

(3) Internal cracking behind the leading edge of the rotor blades has been due to excessive tensile creep strain in this region associated with blade distortion. The presence of cooling passages may have assisted in providing local concentrations of stress from which cracks could originate.

(4) Razor-like trailing edges in both nozzle and rotor blades have led to early chordwise cracking in this region due to their inability to withstand reversals from compressive creep to high tensile stress on turbine 'shut down'. Blade distortion has not influenced cracking in the rotor-blade trailing edges but appears to have aggravated the one chordwise

crack in the nozzle blade. Blade vibration can also aggravate cracking but this does not appear to have been of major significance.

(5) In comparison with the blades examined in this report the general trend in cooled blade design may be towards blades with lower camber and with more rounded and slightly thicker edges. It is fortunate, therefore, that these features will overcome, to some degree, the weak points exhibited by the sintered vitallium blades. A substantial improvement will obviously result from more uniform blade cooling. The present blades, which are a very early design of cooled blade, had particularly poor chordwise distribution of temperature and later designs might be expected to show considerable improvement. Nevertheless, the fact that the present blades, in spite of their obvious deficiencies, endured operation at very high gas temperatures for 100 hours under moderately high stress conditions augurs well for future development of the cooled turbine.

REFERENCES

No.	*Author*	*Title, etc.*
1	D. G. Ainley and N. E. Waldren ..	Investigations on an experimental air-cooled turbine. Part I.—General description of turbine and experimental technique. R. & M. 2975. March, 1954.
2	D. G. Ainley, N. E. Waldren and K. Hughes	Investigations on an experimental air-cooled turbine. Part II.—Cooling characteristics of blades having a multiplicity of small diameter coolant passages. R. & M. 2975. March, 1954.
3	D. E. Fray and N. E. Waldren	Investigations on an experimental air-cooled turbine. Part III.—The effects of cooling on the overall turbine aerodynamic performance and initial operation at an inlet gas temperature of 1400 deg K. (Part III of this report).
4	J. Reeman and R. W. A. Buswell ..	An experimental single stage air-cooled turbine. Part I.—Design of the turbine and manufacture of some experimental internally cooled nozzles and blades. *Proc. I. Mech. E.* Vol. 167. 1953.

APPENDIX I

Blade Details

Turbine annulus, outer diameter = 24 in.

Turbine annulus, inner diameter = 19 in.

All blades of constant section, untwisted and unshrouded.

	Nozzle	*Rotor*
Number of blades	45	99
Blade height	2·5 in.	2·5 in.
Blade chord	2·21 in.	1·05 in.
Thickness/chord	0·1404	0·234
Number of cooling holes per blade	53	38
Size of cooling holes	0·043 × 0·036 in. (elliptical)	0·030 × 0·023 in. (elliptical)
Cross-sectional area contained by profile	0·40 in.^{2}	0·170 in.^{2}
Moment of Inertia of Section		
I min. (parallel to chord)	0·00575 in.^{4}	0·00126 in.^{4}
Distance chord to neutral axis	0·258 in.	0·236 in.
I max. (normal to chord)	0·598 in.^{4}	
Distance L.E. to neutral axis..	0·912 in.	

(For further details *see* Ref. 2)

APPENDIX II

Properties of Sintered Tungsten Vitallium Alloy

Chemical Composition

Nominal ..	64% Cobalt	30% Chromium	6% Tungsten
Typical ..	63·5% Cobalt	29% Chromium	6·4% Tungsten
	0·13% Iron	0·27% Aluminium	0·22% Silicon
	0·024% Carbon		

Density .. lb/cu in. at 20 deg C rotor 0·305, nozzle 0·299 (theoretical 0·308)

Mean thermal expansion in./in./°C × 10^6

21°C to 537°C = 14·3
21°C to 649°C = 15·2
21°C to 815°C = 16·3
21·C to 868°C = 16·7
21°C to 980°C = 17·9
815°C = 17·7
980°C = 21·0

Melting point	1420°C
Hardness (VPN −30 Kg)	320 to 350
Izod impact value, ft/lb	8

	R.T.	650 °C	750 °C	850 °C
Ultimate tensile strength, tons/sq in.	44·5	—	34·5	21
Yield strength tons/sq in.	35·5	—	22·5	15
Elongation per cent on 0·625 in.	6·1	—	7·5	10·5
Young's modulus lb/sq in. × 10^{-6}	—	24	18	—
Stress for fatigue fracture in 300 hours (Haigh machine) tons/sq in.			±10·5	± 6·5
Stress to fracture under steady load				
in 10 hours tons/sq in.			17·5	
in 100 hours tons/sq in.			12·5	
in 1000 hours tons/sq in.			7·5	

Scaling factor	750 °C	950 °C	1100 °C
(Mgm/sq cm of scale removed by sodium hydride process after 70 hours at temperature in moist air)..	0·23	0·9	3·4

(78656) D

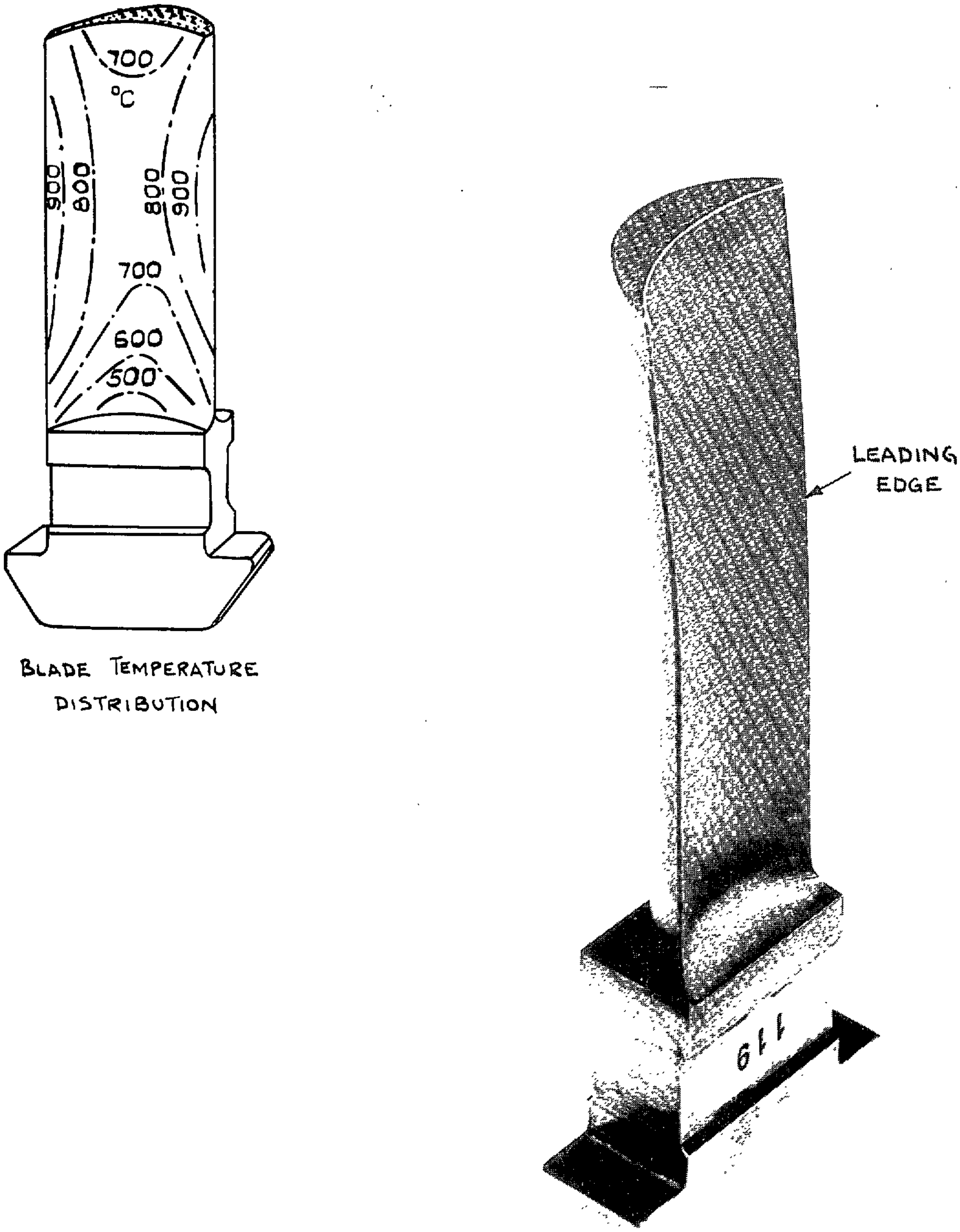

FIG. 1. Typical distortion in rotor blades.

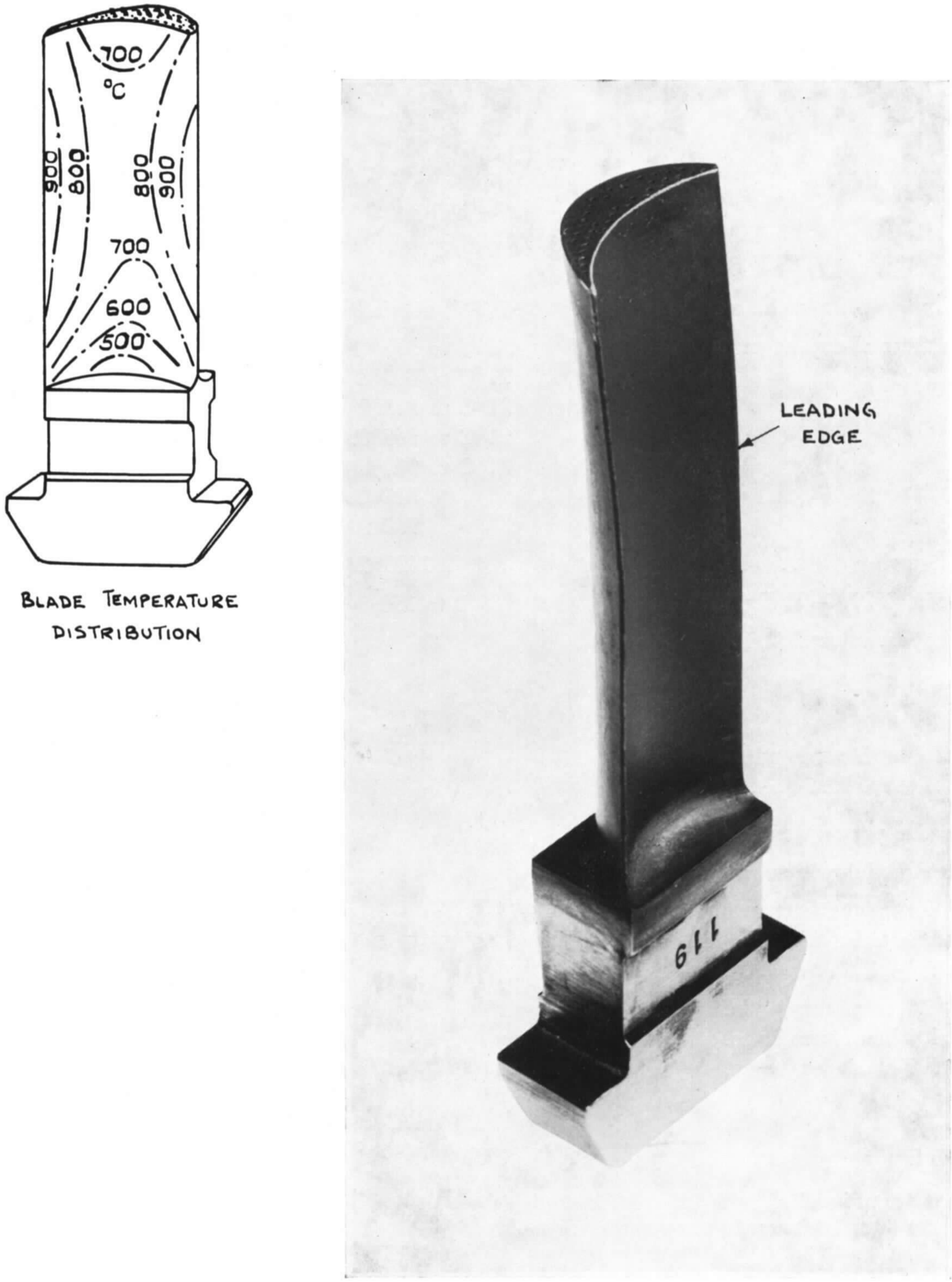

FIG. 1. Typical distortion in rotor blades.

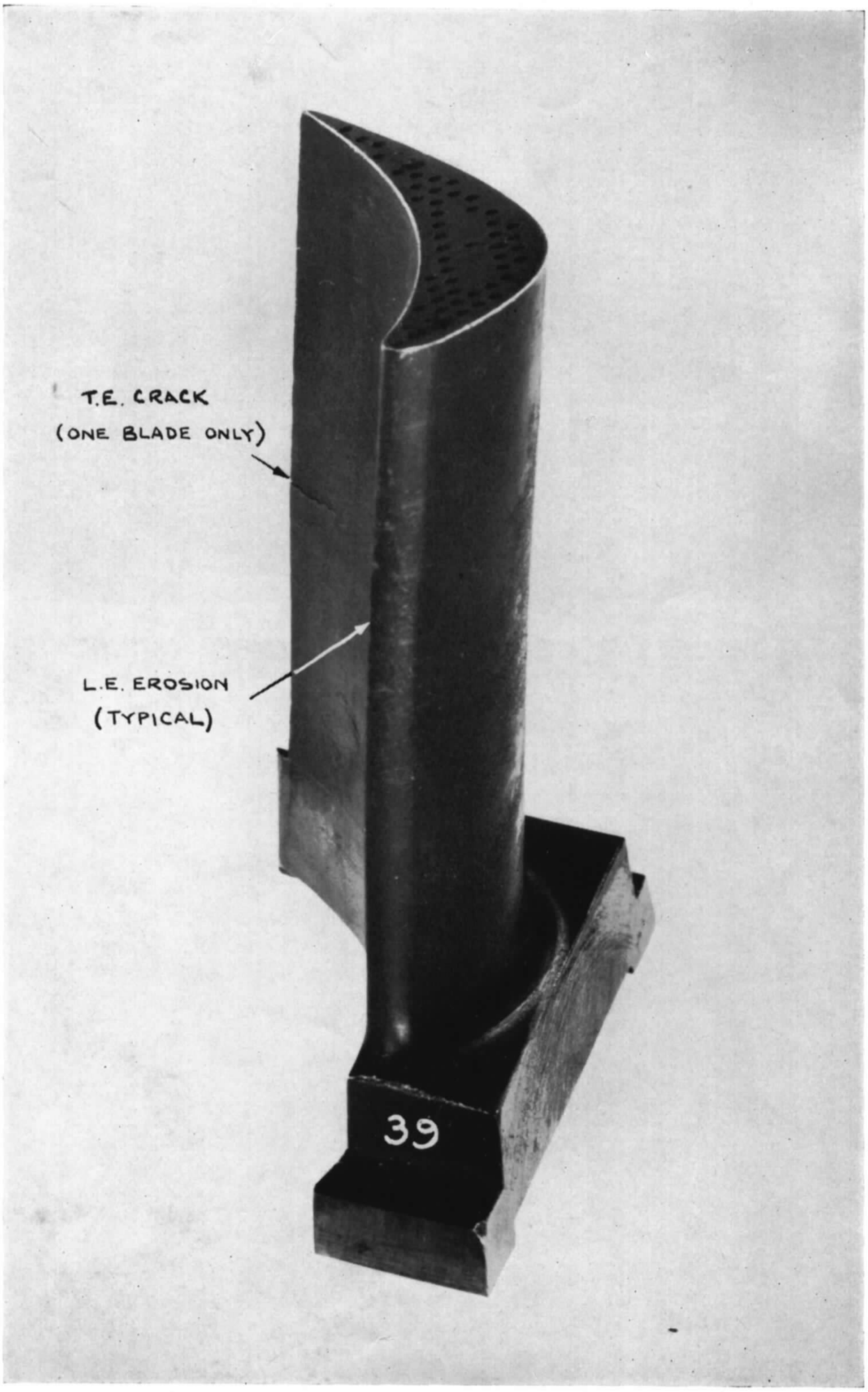

FIG. 2. Typical distortion in nozzle blades.

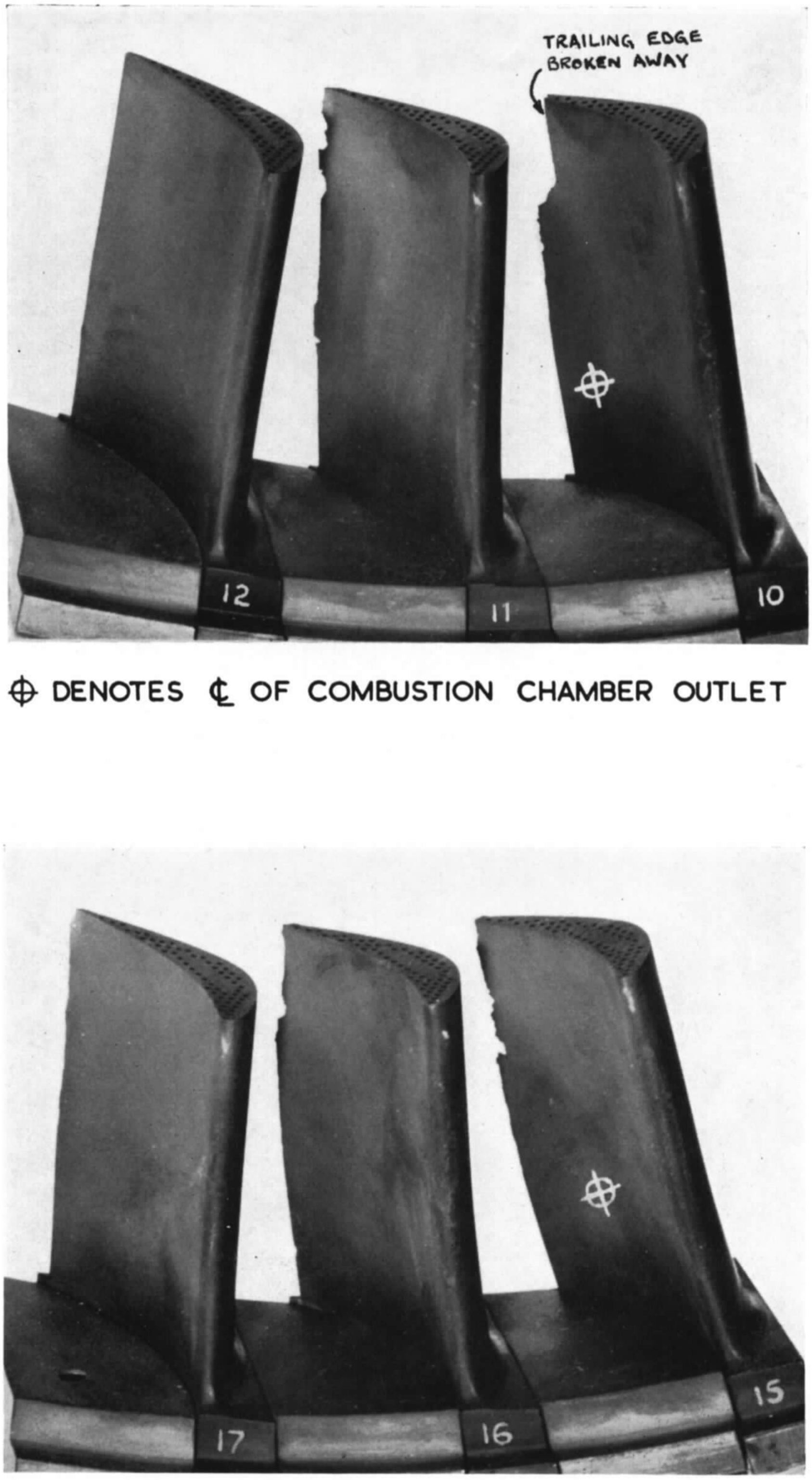

FIG. 3. Damage to nozzle-blade trailing edges.

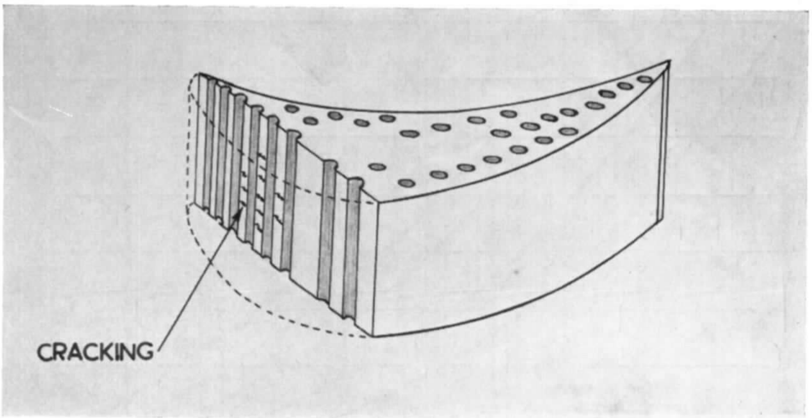

BLADE Nº 119 SECTION AT MID-SPAN

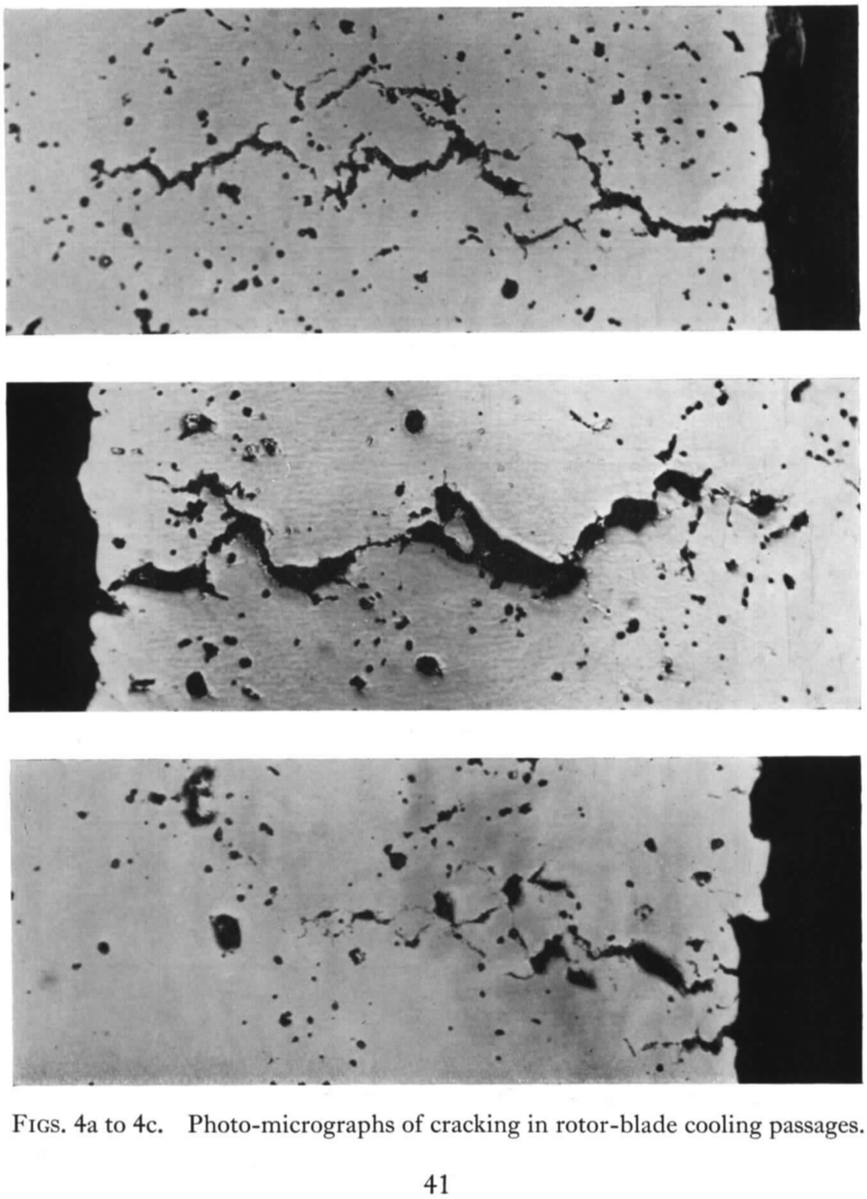

(a)

(b)

(c)

FIGS. 4a to 4c. Photo-micrographs of cracking in rotor-blade cooling passages.

(78656)

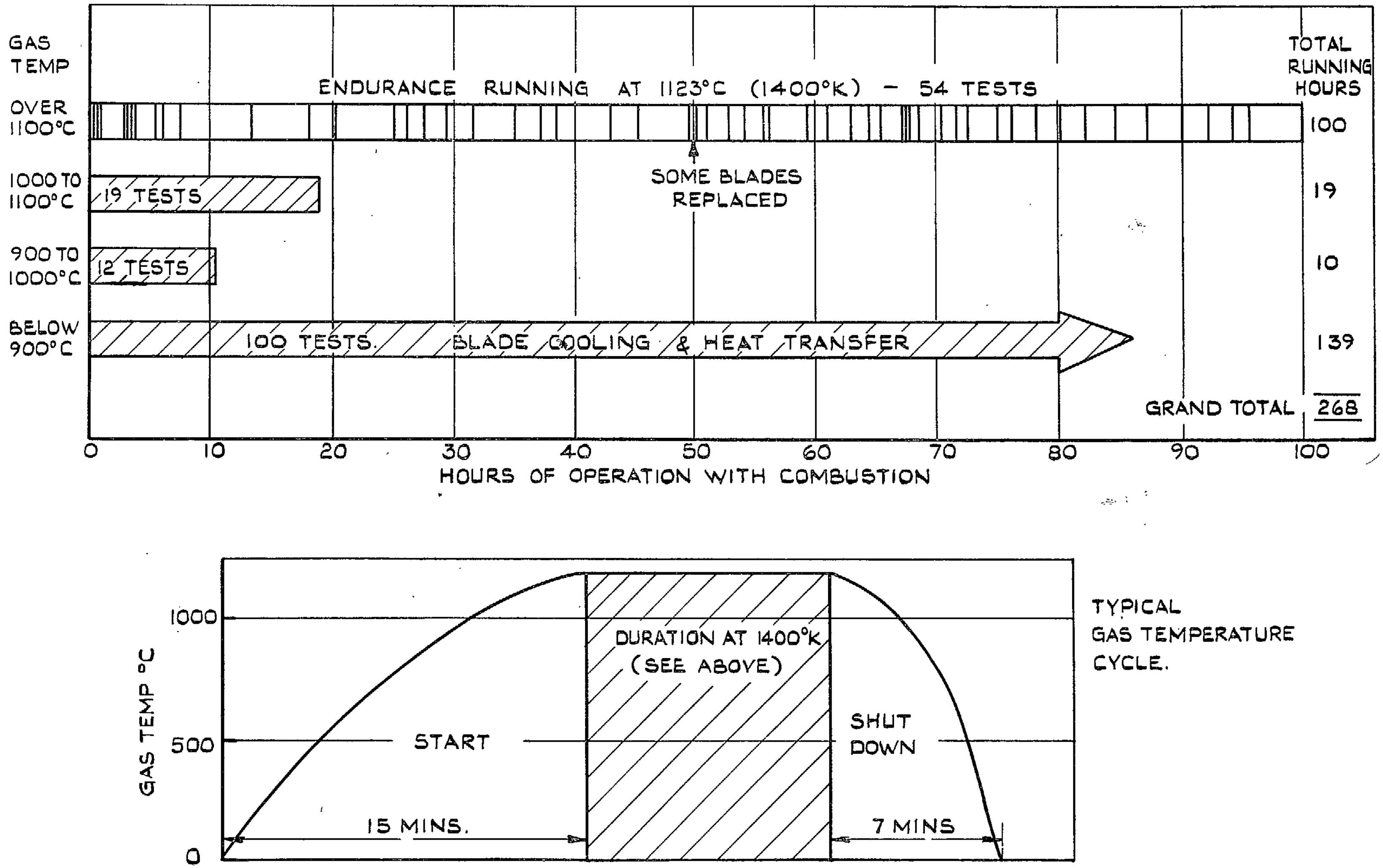

FIG. 6. Turbine running hours.

E

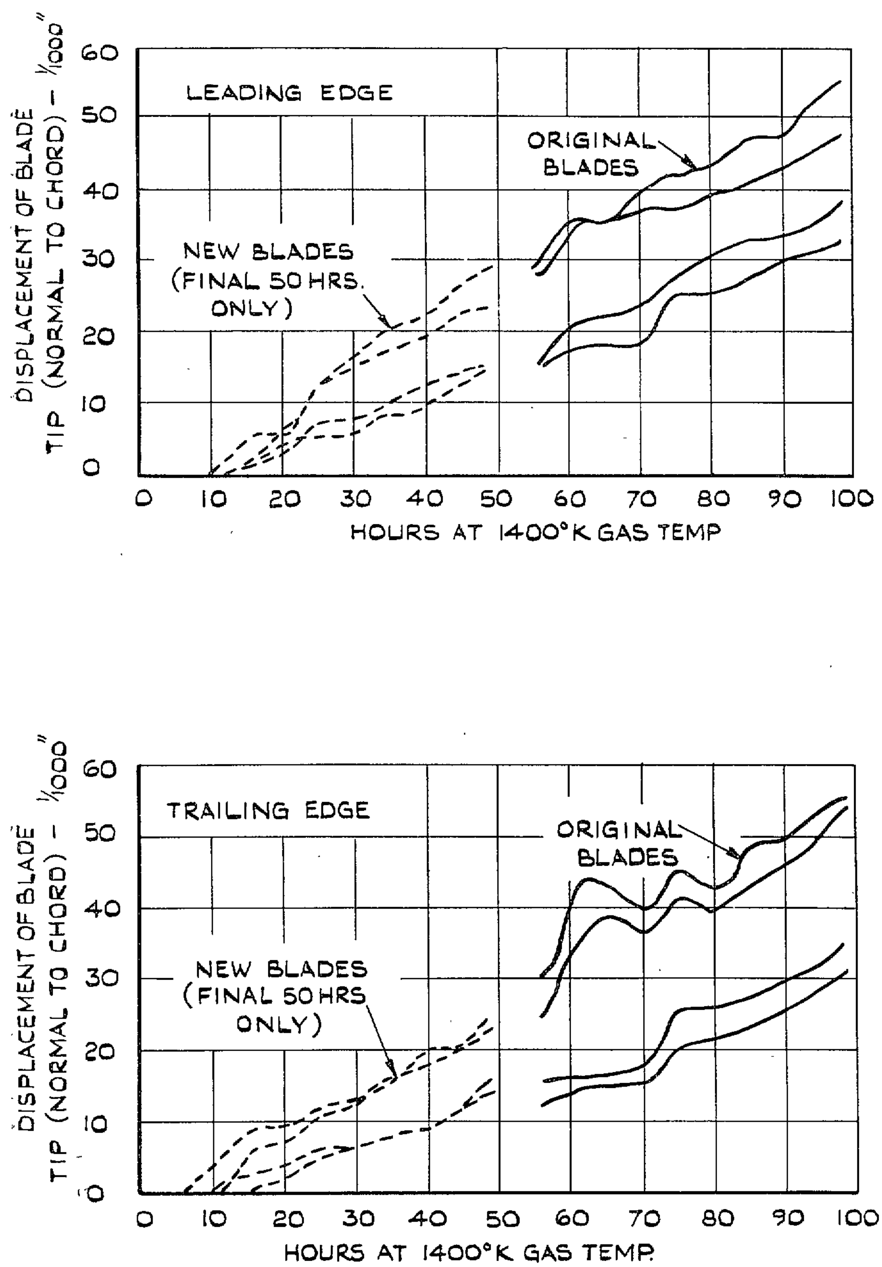

FIG. 7. Progressive distortion in rotor blades.

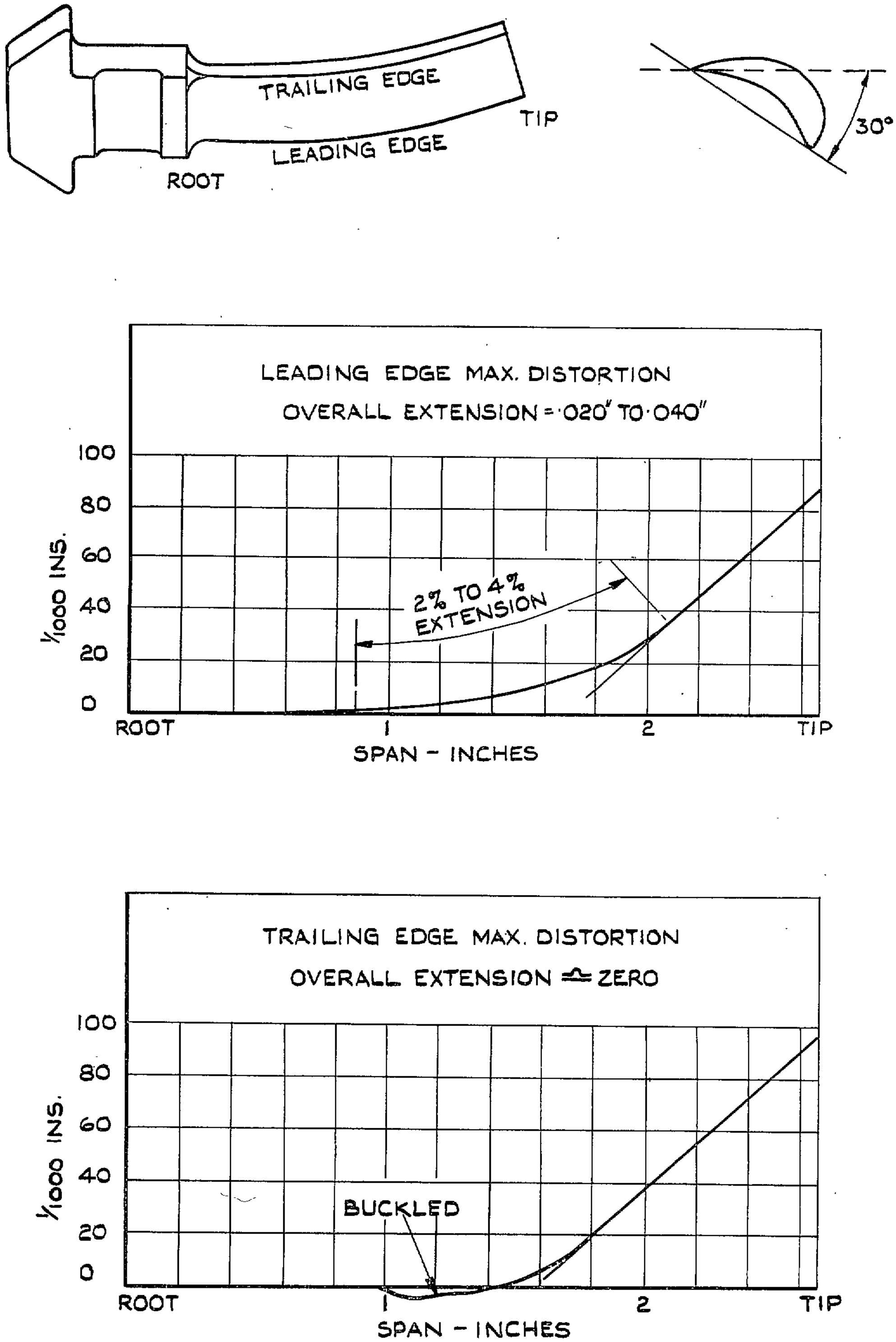

FIG. 8. Typical distortion in rotor-blade leading and trailing edges.

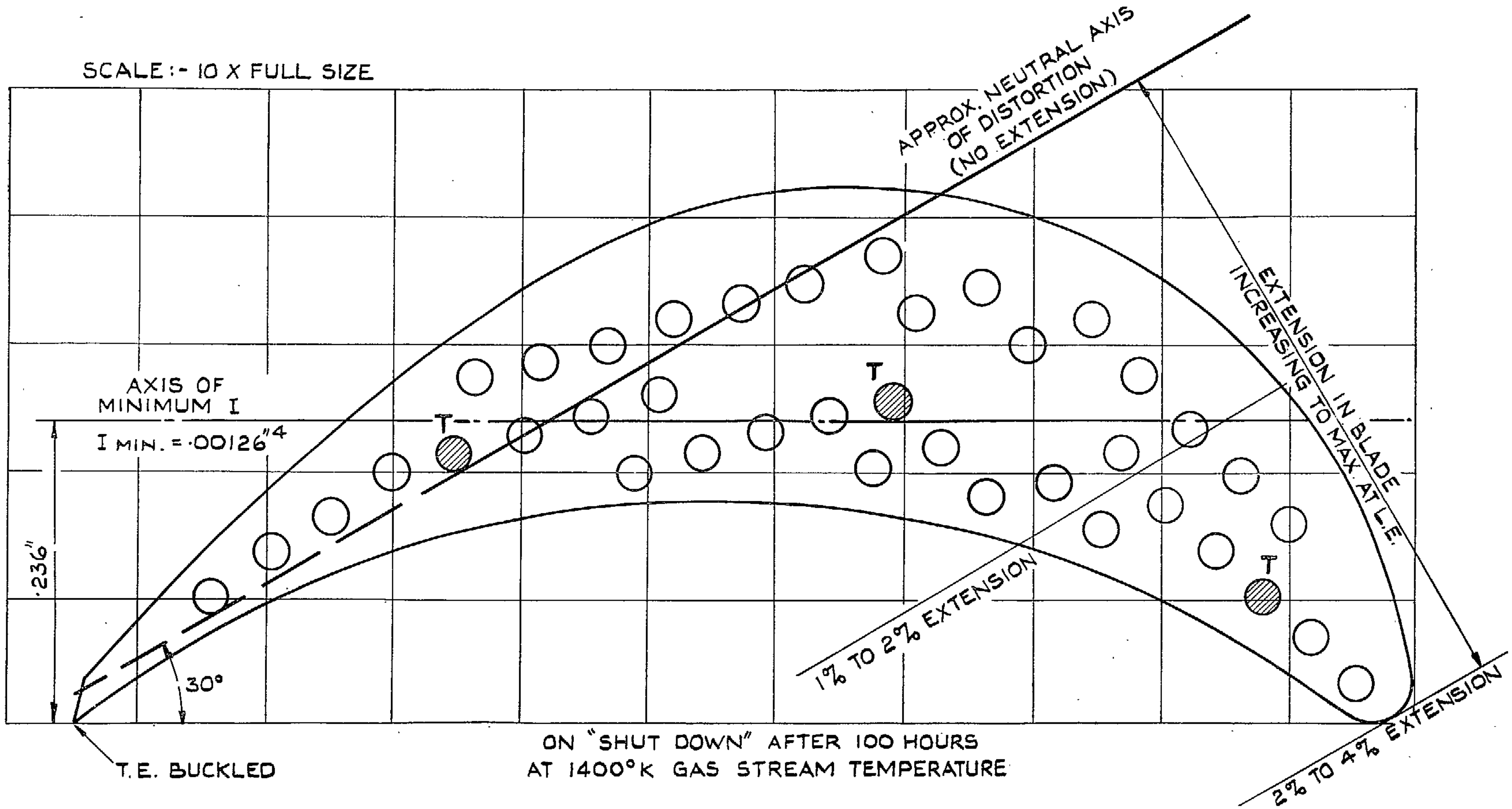

FIG. 9. Analysis of rotor-blade distortion at weakest point in span.

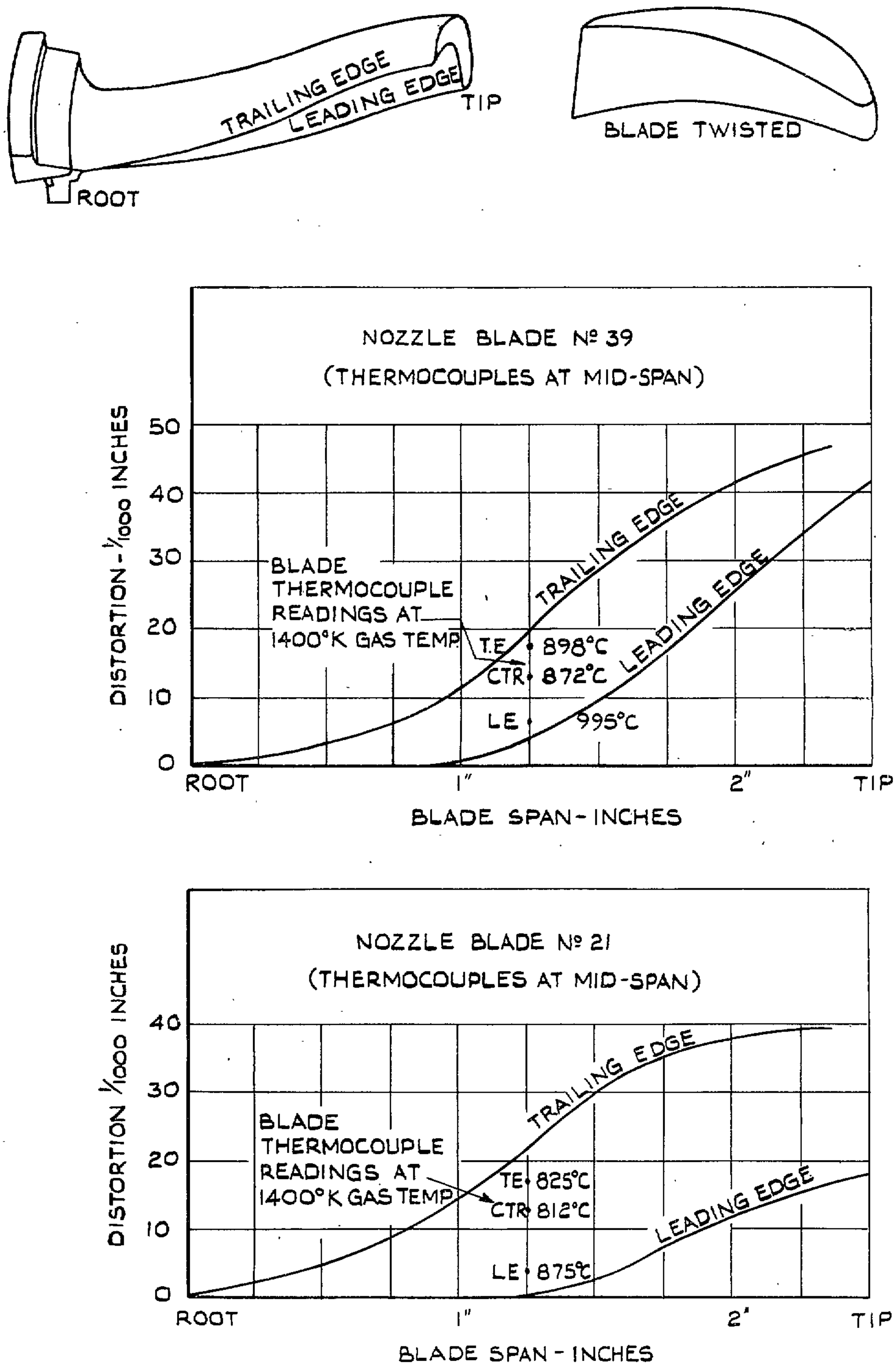

FIG. 10. Typical distortion in nozzle-blade leading and trailing edges.

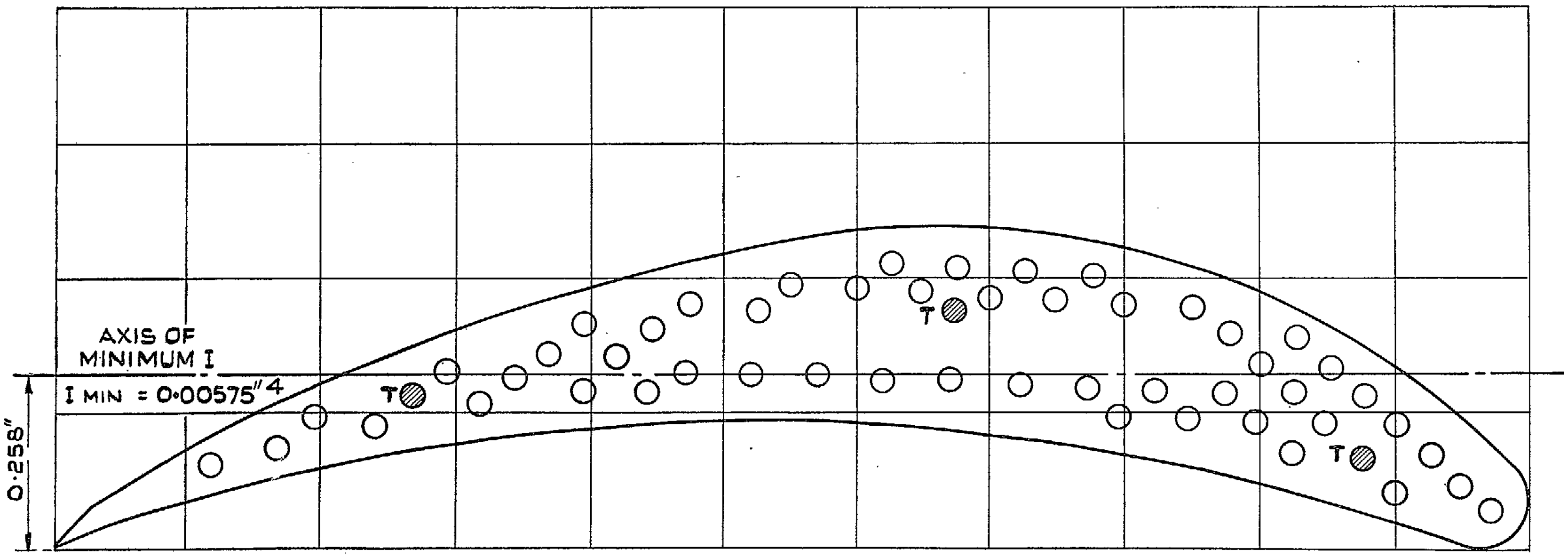

FIG. 11. Chordwise section through nozzle blade.

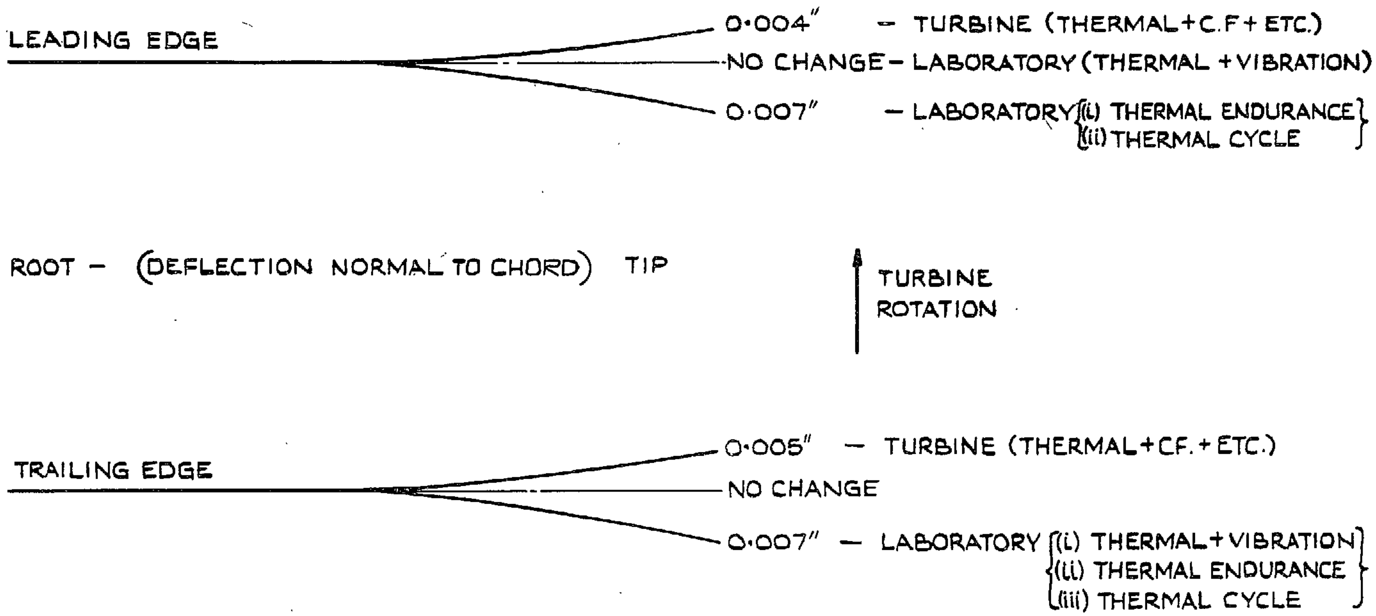

FIG. 12. Comparison between rotor-blade distortion in turbine and laboratory over 20-hour period.

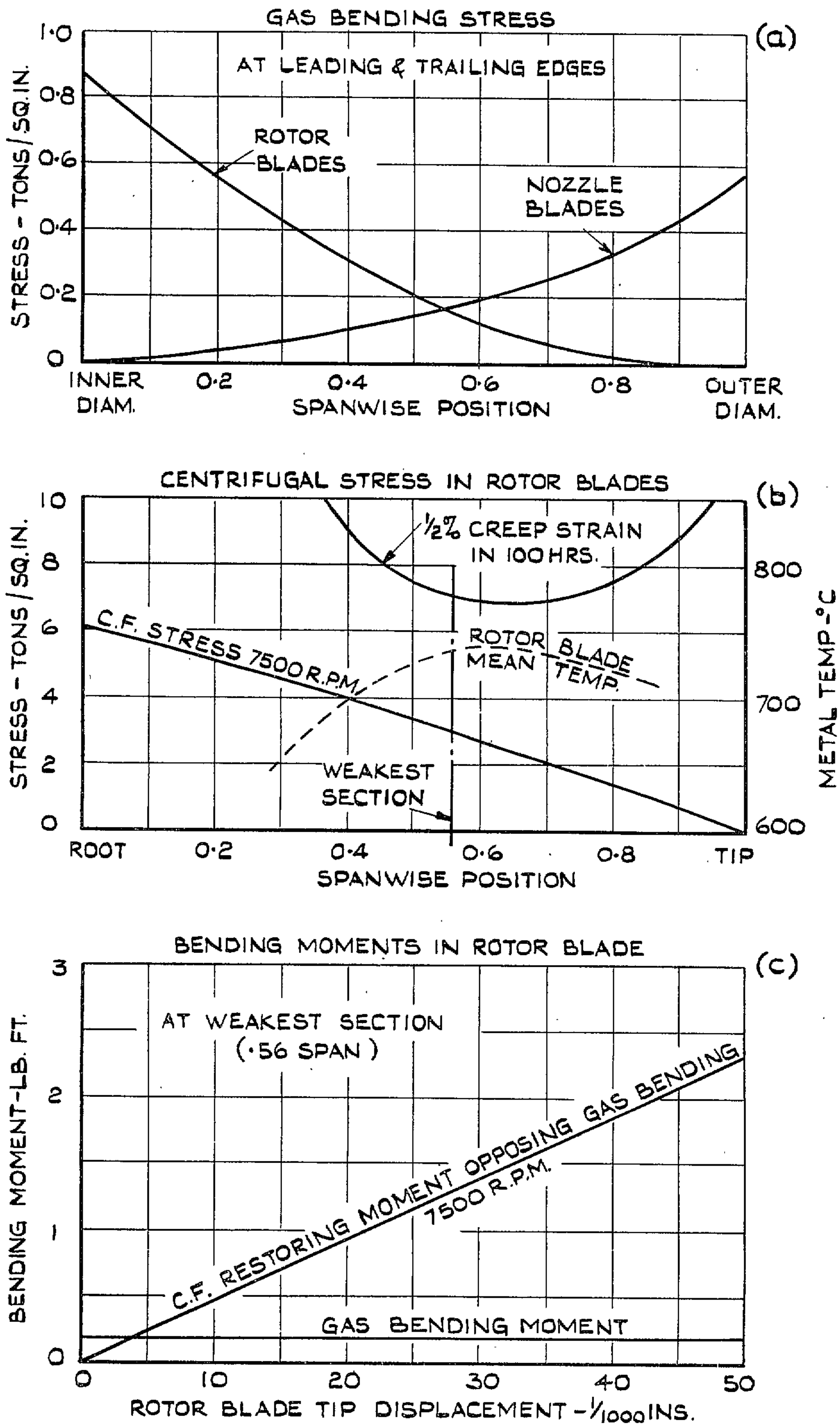

FIG. 13a to 13c. Gas bending and centrifugal stresses in blades.

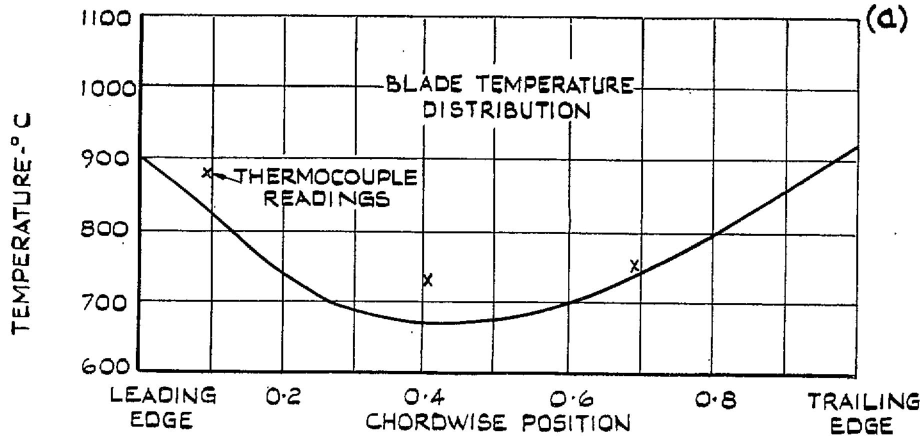

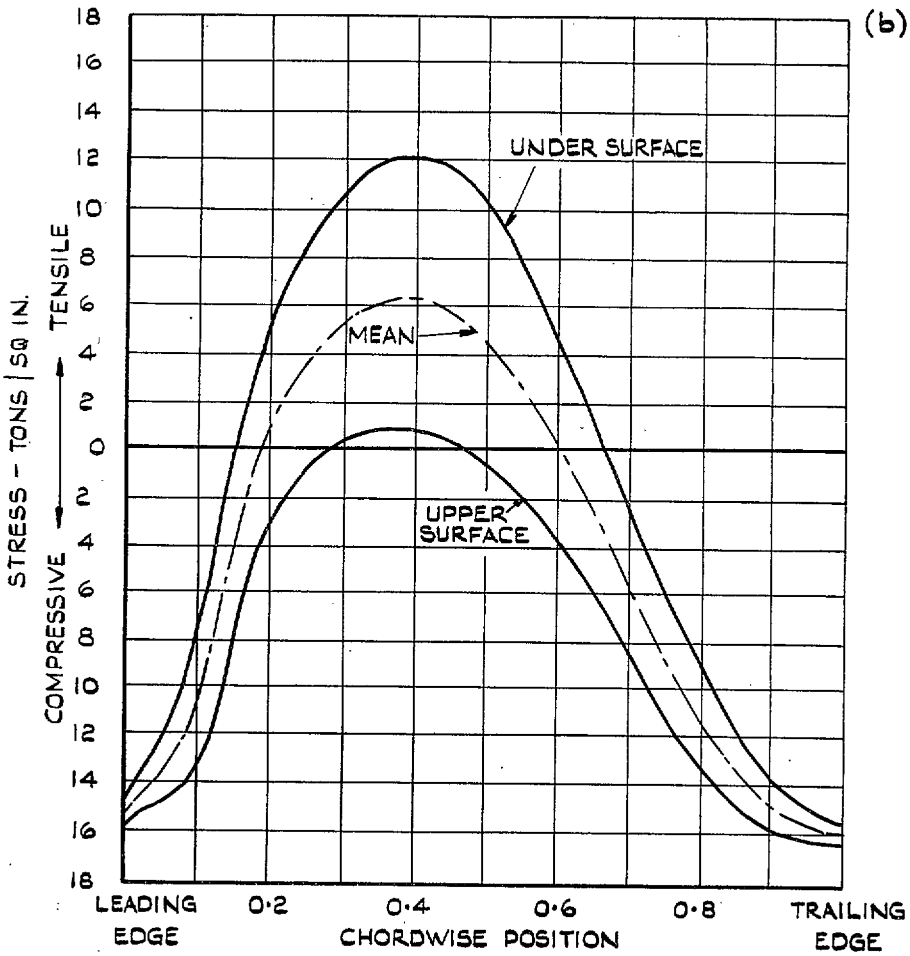

FIGS. 14a and 14b. Estimated direct thermal stresses in weakest section of rotor-blade span (No yield).

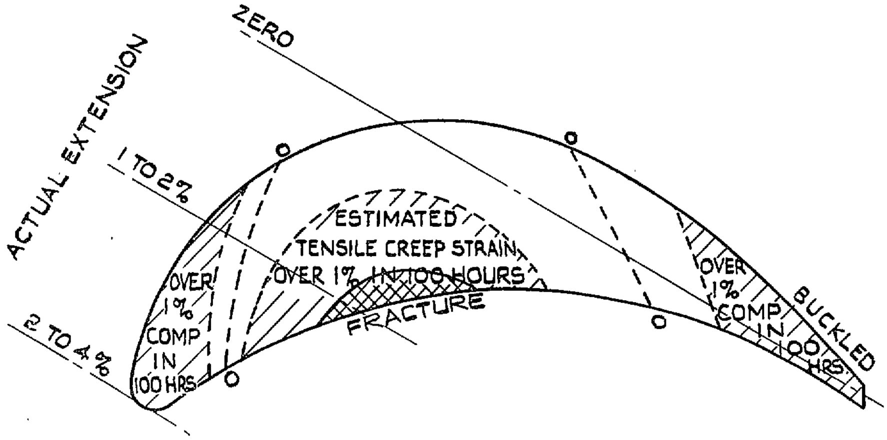

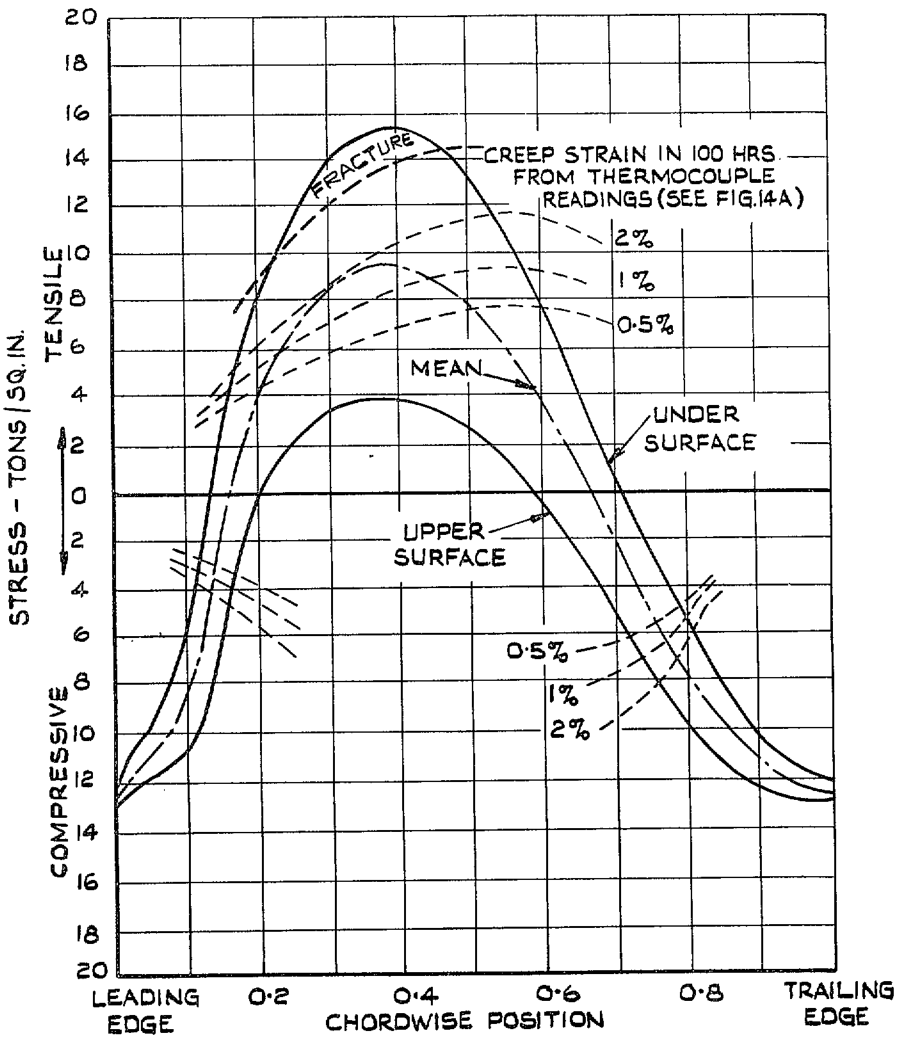

FIG. 15. Combined thermal and centrifugal stresses in weakest section of rotor-blade span (No yield).

(78656) Wt. 54/8210 K.6 9/60 Hw.

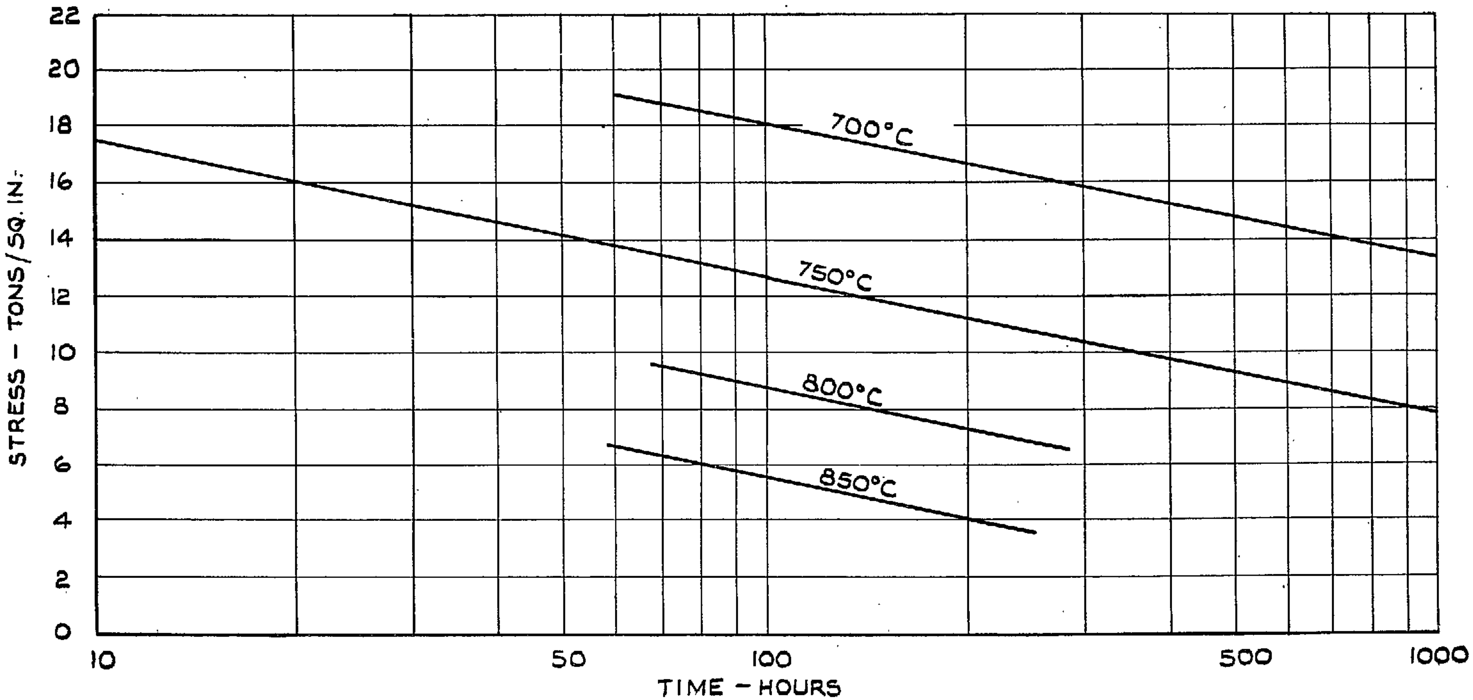

FIG. 16. Stress to rupture vs. time for sintered tungsten vitallium alloy.

Publications of the Aeronautical Research Council

ANNUAL TECHNICAL REPORTS OF THE AERONAUTICAL RESEARCH COUNCIL (BOUND VOLUMES)

1941 Aero and Hydrodynamics, Aerofoils, Airscrews, Engines, Flutter, Stability and Control, Structures. 63*s.* (post 2*s.* 3*d.*)

1942 Vol. I. Aero and Hydrodynamics, Aerofoils, Airscrews, Engines. 75*s.* (post 2*s.* 3*d.*)
Vol. II. Noise, Parachutes, Stability and Control, Structures, Vibration, Wind Tunnels. 47*s.* 6*d.* (post 1*s.* 9*d.*)

1943 Vol. I. Aerodynamics, Aerofoils, Airscrews. 80*s.* (post 2*s.*)
Vol. II. Engines, Flutter, Materials, Parachutes, Performance, Stability and Control, Structures. 90*s.* (post 2*s.* 3*d.*)

1944 Vol. I. Aero and Hydrodynamics, Aerofoils, Aircraft, Airscrews, Controls. 84*s.* (post 2*s.* 6*d.*)
Vol. II. Flutter and Vibration, Materials, Miscellaneous, Navigation, Parachutes, Performance, Plates and Panels, Stability, Structures, Test Equipment, Wind Tunnels. 84*s.* (post 2*s.* 6*d.*)

1945 Vol. I. Aero and Hydrodynamics, Aerofoils. 130*s.* (post 2*s.* 9*d.*)
Vol. II. Aircraft, Airscrews, Controls. 130*s.* (post 2*s.* 9*d.*)
Vol. III. Flutter and Vibration, Instruments, Miscellaneous, Parachutes, Plates and Panels, Propulsion. 130*s.* (post 2*s.* 6*d.*)
Vol. IV. Stability, Structures, Wind Tunnels, Wind Tunnel Technique. 130*s.* (post 2*s.* 6*d.*)

Special Volumes

Vol. I. Aero and Hydrodynamics, Aerofoils, Controls, Flutter, Kites, Parachutes, Performance, Propulsion, Stability. 126*s.* (post 2*s.* 6*d.*)
Vol. II. Aero and Hydrodynamics, Aerofoils, Airscrews, Controls, Flutter, Materials, Miscellaneous, Parachutes, Propulsion, Stability, Structures. 147*s.* (post 2*s.* 6*d.*)
Vol. III. Aero and Hydrodynamics, Aerofoils, Airscrews, Controls, Flutter, Kites, Miscellaneous, Parachutes, Propulsion, Seaplanes, Stability, Structures, Test Equipment. 189*s.* (post 3*s.* 3*d.*)

Reviews of the Aeronautical Research Council

1939–48 3*s.* (post 5*d.*) 1949–54 5*s.* (post 6*d.*)

Index to all Reports and Memoranda published in the Annual Technical Reports

1909–1947 R. & M. 2600 6*s.* (post 4*d.*)

Author Index to the Reports and Memoranda and Current Papers of the Aeronautical Research Council

February, 1954–February, 1958 R & M. No. 2570 (Revised) (Addendum) 7*s.* 6*d.* (post 4*d.*)

Indexes to the Technical Reports of the Aeronautical Research Council

July 1, 1946–December 31, 1946 R. & M. No. 2150 1*s.* 3*d.* (post 2*d.*)

Published Reports and Memoranda of the Aeronautical Research Council

Between Nos. 2251–2349	R. & M. No. 2350	1*s.* 9*d.* (post 2d.)
Between Nos. 2351–2449	R. & M. No. 2450	2*s.* (post 2*d.*)
Between Nos. 2451–2549	R. & M. No. 2550	2*s.* 6*d.* (post 2*d.*)
Between Nos. 2551–2649	R. & M. No. 2650	2*s.* 6*d.* (post 2*d.*)
Between Nos. 2651–2749	R. & M. No. 2750	2*s.* 6*d.* (post 2*d.*)
Between Nos. 2751–2849	R. & M. No. 2850	2*s.* 6*d.* (post 2*d.*)
Between Nos. 2851–2949	R. & M. No. 2950	3*s.* (post 2*d.*)

HER MAJESTY'S STATIONERY OFFICE

from the addresses overleaf

Printed and published by
HER MAJESTY'S STATIONERY OFFICE

To be purchased from
York House, Kingsway, London W.C.2
423 Oxford Street, London W.1
13A Castle Street, Edinburgh 2
109 St. Mary Street, Cardiff
39 King Street, Manchester 2
Tower Lane, Bristol 1
2 Edmund Street, Birmingham 3
80 Chichester Street, Belfast 1
or through any bookseller

Printed in England

R. & M. No. 3144

S.O. Code No. 23-3144